Petunia hybrida PDR2 is involved in herbivore defense by controlling steroidal contents in trichomes

Sasse, Joëlle ; Schlegel, Markus ; Borghi, Lorenzo ; Ullrich, Friederike ; Lee, Miyoung ; Liu, Guo-Wei ; Giner, José-Luis ; Kayser, Oliver ; Bigler, Laurent ; Martinoia, Enrico ; Kretzschmar, Tobias

Abstract: As a first line of defense against insect herbivores many plants store high concentrations of toxic and deterrent secondary metabolites in glandular trichomes. Plant Pleiotropic Drug Resistance (PDR)-type ABC transporters are known secondary metabolite transporters, and several have been implicated in pathogen or herbivore defense. Here, we report on Petunia hybrida PhPDR2 as a major contributor to trichome-related chemical defense. PhPDR2 was found to localize to the plasma membrane and be predominantly expressed in multicellular glandular trichomes of leaves and stems. Down-regulation of PhPDR2 via RNA interference (pdr2) resulted in a markedly higher susceptibility of the transgenic plants to the generalist foliage feeder Spodoptera littoralis. Untargeted screening of pdr2 trichome metabolite contents showed a significant decrease in petuniasterone and petuniolide content, compounds, which had previously been shown to act as potent toxins against various insects. Our findings suggest that PhPDR2 plays a leading role in controlling petuniasterone levels in leaves and trichomes of petunia, thus contributing to herbivory resistance.

DOI: https://doi.org/10.1111/pce.12828

Title page

Petunia hybrida PDR2 is Involved in Herbivore Defense by Controlling Steroidal Contents in Trichomes

Joëlle Sasse[1], Markus Schlegel[1&], Lorenzo Borghi[1&], Friederike Ullrich[3], Miyoung Lee[1], Guo-Wei Liu[1], José-Luis Giner[4], Oliver Kayser[3], Laurent Bigler[2*], Enrico Martinoia[1*], and Tobias Kretzschmar[1, 5,*]

[1]Institute of Plant Biology, University of Zurich, Zurich, Switzerland

[2]Department of Chemistry, University of Zurich, Zurich, Switzerland

[3]Department of Biochemical and Chemical Engineering, TU Dortmund, Dortmund, Germany

[4]Department of Chemistry, SUNY-ESF, Syracuse, NY, USA

[5]International Rice Research Institute, Metro-Manila, Philippines

[&] equally contributing second authors

[*]Correspondence: t.kretzschmar@irri.org; laurent.bigler@chem.uzh.ch

Abstract

As a first line of defense against insect herbivores many plants store high concentrations of toxic and deterrent secondary metabolites in glandular trichomes. Plant Pleiotropic Drug Resistance (PDR)-type ABC transporters are known secondary metabolite transporters and several have been implicated in pathogen or herbivore defense. Here, we report on *Petunia hybrida* PhPDR2 as a major contributor to trichome-related chemical defense. PhPDR2 was found to localize to the plasma membrane and be predominantly expressed in multicellular glandular trichomes of leaves and stems. Downregulation of *PhPDR2* via RNA interference (*pdr2*) resulted in a markedly higher susceptibility of the transgenic plants to the generalist foliage feeder *Spodoptera littoralis*. Untargeted screening of *pdr2* trichome metabolite contents showed a significant decrease in petuniasterone and petuniolide content, compounds, which had previously been shown to act as potent toxins against various insects. Our findings suggest that PhPDR2 plays a leading role in controlling petuniasterone levels in leaves and trichomes of petunia, thus contributing to herbivory resistance.

Keywords:

Petunia, ABC transporter, Glandular trichome, Herbivory, Secondary metabolism, metabolomics

Introduction

Over a million insect species are estimated to feed on terrestrial plants (Howe and Jander 2008), and insect pests have been causing crop losses since the dawn of agriculture (Oerke 2005). Through 400 million years of co-evolution plants developed a number of constitutive and inducible defense responses to cope with insect herbivory. Wax depositions on plant surfaces, foliar defense compounds, and leaf hairs (trichomes) are examples for constitutive defenses against biotic stressors (Howe and Jander 2008). Examples of inducible responses include the production of protease inhibitors that impede digestion, the release of volatiles that attract specific predators, and the synthesis and activation of toxins (Bodenhausen and Reymond 2007). Toxins and deterrents are often produced and stored in trichomes (Howe and Jander 2008; Bleeker et al. 2012).

Trichomes are uni- or multicellular epidermal protrusions that are formed on aerial parts of plants (Wagner 1991) and are broadly classified into being either non-glandular or glandular. Glandular trichomes consist of a bulbous head on top of stalk cells (Wagner 1991), which is loaded with secondary metabolites. The head is separated from the environment by a cuticule layer only, which bursts easily on contact with an herbivore to release its contents (Wagner 1991). Glandular trichomes are of demonstrated importance in herbivory defense as exemplified by *Datura wrightii*, a species with trichome bimorphism. The variety producing glandular trichomes was observed to be more resistant to herbivory than the variety that produces exclusively non-glandular trichomes (van Dam and Hare 1998; Hare 2005). Glandular trichomes are highly specialized on the production and storage of secondary metabolites, which can make up to 10-15% of the leaf dry weight (Wagner et al. 2004).

A plethora of secondary metabolites, among them multiple alkaloids, terpenes, polyketides, and phenolics are believed to have evolved primarily as means of defense and many of them are trichome specific (Wang et al. 2001; Yazaki 2006; Schilmiller et al. 2008; Slocombe et al. 2008; Loreto et al. 2014). Terpenes constitute the largest group of secondary metabolites with over 25,000 known structures that include toxins and deterrents against bacteria, fungi, and animals (Gershenzon and Dudareva 2007). Terpenoid metabolism is highly active in glandular trichomes of many species including Solanaceae (Besser et al. 2009; Bleeker et al. 2012; Tissier et al. 2013). Cembranoids, a group of diterpenes in a tobacco variety were shown to accumulate to approximately 10% of leaf dry weight and 60% of the trichome exudate weight (Wang et al. 2001; Wang and Wagner 2003).

Many secondary metabolites are potentially harmful to the plant itself (Cutler et al. 1977; Howe and Jander 2008) and thus, plants have developed strategies to avoid autointoxication. Some highly toxic compounds are only fully synthesized upon attack or stored as conjugated inert molecules until activated upon tissue wounding. Many defense compounds are either stored within vacuoles or secreted into the apoplast, places that are not connected to the plant's primary metabolism. On tissue level they are stored in specialized organs such as glandular trichomes, laticifers or secretory ducts. Indeed, apart from import of energy-rich compounds and precursors for specialized biosynthetic pathways, trichome metabolism is largely disconnected from the rest of the plant metabolism (Schilmiller et al. 2008). However, many compounds such as terpenoids, are hydrophobic and tend to diffuse across membranes along their concentration gradient. To avoid toxic effects due to reflux, steep concentration

92 gradients have to be maintained between sites of synthesis and storage that likely
93 depend on the existence of energy-dependent transporters.
94 Transporters that directly utilize adenosine triphosphate (ATP) as an energy source are
95 more efficient in establishing and maintaining steep concentration gradients than those
96 relying on electrochemical gradients (Kreuz et al. 1996) Thus, proteins of the ATP
97 binding cassette (ABC) family (Kang et al. 2011; Yazaki 2006) are primary candidates to
98 create and maintain the postulated strong gradients between trichomes and leaves or
99 trichome heads and stalk cells. ABC proteins are present in all kingdoms, from bacteria
100 to humans (Theodoulou 2000), but they are most abundant and diversified in plants.
101 ABC members of the ABCG subfamily have been reported to be involved in lipid and
102 phytohormone transport, biotic stress responses of plants and in transport of secondary
103 metabolites (Kang et al. 2011; Kretzschmar et al. 2012; Banasiak et al. 2013, Hwang et
104 al. 2016). Many full-size ABCG members, also termed Pleiotropic Drug Resistance
105 (PDR) proteins, are transcriptionally responsive to pathogen elicitors and jasmonic acid
106 treatment (Kretzschmar et al. 2011). NtPDR1 and NpPDR1 were furthermore
107 demonstrated to be expressed in glandular trichomes (Sasabe et al. 2002; Crouzet et al.
108 2013; Stukkens et al. 2005) and involved in transport of the fungi-toxic diterpene sclareol
109 (Cutler et al. 1977; Jasinski et al. 2001; Crouzet et al. 2013). NtPDR5 was described as
110 responsive to herbivory, its expression being induced upon jasmonic acid treatment,
111 mechanical wounding, and feeding by the Solanaceae specialist *Manduca sexta*
112 (Bienert et al. 2012). However, potential substrates of this transporter remain unknown.
113 Collectively PDR proteins are plasma membrane intrinsic secondary metabolite
114 transporters that have been found in trichomes, making them excellent candidates for
115 cellular export of deterrents and toxins related to herbivory. We performed our analysis

116 in petunia, which serves as a Solanaceae model species (Gerats and Vandenbussche
117 2005) and has leaves that are highly toxic to herbivores. Here, we report on PhPDR2,
118 which localizes to glandular trichomes of petunia leaf and stem tissue and is involved in
119 herbivore defense presumably through modulation of insecticidal steroidal compounds.
120

Methods

Plant growth conditions: All experiments were performed with *Petunia hybrida* cultivar W115. Plants were grown under long day conditions with 16 h of continuous light at 40% relative humidity. Plants were either grown on soil (ED 73 Einheitserde) or on clay granules (Oil Dry US Special from Damolin) supplemented once a week with 1x Hoagland solution. On plate, plants were grown on medium containing 2.2 g L^{-1} MS (Duchefa) and with or without 15 g L^{-1} sucrose (0.5 MS - Suc, 0.5 MS + Suc plates, respectively), supplemented with 9 g L^{-1} phyto agar (Duchefa) at 16 h of light and 25 °C.

Conserved *PDR* domain amplification: For the investigation of petunia *PDR* sequences expressed in leaf and trichome tissue, primers were designed on a CDS alignment of *PDRs* from different Solanaceae. *Solanum lycopersicum* sequences were obtained from a Blast of *PhPDR2* and *PDR1* against the tomato database (http://mips.helmholtz-muenchen.de/plant/tomato/database). The search resulted in 23 hits listed in the Accession Numbers section. *Solanum tuberosum* CDS were obtained from GenBank for *StPDR1* – *StPDR4*, and by a Blast search with *PDR1* and *PhPDR2* against the *Solanum tuberosum* database (http://solgenomics.net/organism/Solanum_tuberosum/genome), which resulted in 29 hits listed in the Accession Numbers section. Furthermore, the *Nicotiana plumbaginifolia* CDS of *NpPDR1*, *NpPDR2*, *NpPDR3*, *NpPDR5*, the *Nicotiana tabacum NtPDR1*, *NtPDR3*, *NtPDR4*, *NtPDR5a*, and *NtPDR5b* were included. The Walker A box of NBD 2 and the PDR signature 4 were part of the most conserved part of the alignment. Thus, PCR was performed on this region (F 5'-agcwytrrtgggwgtyagtggdgctgg, R 5'-ctcatcaaadgcttcaaawatgtc) and the fragments were cloned into pGEM®-T easy vector (Promega, USA), sequenced and aligned with the MultAlin software

(http://multalin.toulouse.inra.fr/multalin/). Fragments that were only amplified once were excluded from the analysis.

***PhPDR2* phylogenetic analysis:**

To set PhPDR2 in relation to described PDR proteins, the well-established *Oryza sativa* and the *A. thaliana* PDR proteins, as well as *Spirodela polyrrhiza SpTUR2*, *Glycine max GmPDR12*, the *N. plumbaginifola NpPDR1, NpPDR2, NpPDR3, NpPDR5*, the *N. tabacum NtPDR1, NtPDR3, NtPDR4, NtPDR5a, NtPDR5b,* the *Petunia hybrida* PDR1 were included in the analysis. PDR Clusters were annotated after Crouzet et. al, 2005. The conserved region (see Conserved domain analysis) of the respective genes was identified and phylogeny of the 0.5 kb fragments was analyzed with a maximum-likelihood tree created on Phylogeny.fr (http://www.phylogeny.fr/)(Dereeper et al. 2008). with the following settings: 16 maximal iterations in MUSCLE alignment, minimal block length of 10 and no gap positions in Gblocks 0.91b alignment refinement (Dereeper et al. 2008).

***PhPDR2* transcriptional induction and quantitative PCR:** For hormone and elicitor treatment 14 d old W115 seedlings grown on plate were exposed for 24 h with final concentrations of 100 µM salicylic acid (SA), 0.1 ml L^{-1} methyl-jasmonate (MJa), 10 g L^{-1} yeast extract, 10 µM abscisic acid (ABA), 25 µM 1-naphthaleneacetic acid (NAA), or 500 µM sclareol.

RNA was isolated with the RNeasy Plant Mini Kit (Qiagen USA) and reverse transcribed to cDNA with M-MLV Reverse Transcriptase (Promega, USA). Quantitative PCR was performed with 5'-TCAAGGCATTCAACTTCCAG and 5'-TACTGACCGAGTCTCCACCA for *PhPDR2* transcription level detection in seedlings and in various tissues. Glyceraldehyde-3-phosphate dehydrogenase (GapDH) served as a housekeeping gene,

and was amplified with 5’-GACTGGAGAGGTGGAAGAGC and 5’-CCGTTAAGAGCTGGGAGAAC. All reactions were performed in SYBR Green PCR Master Mix (Applied Biosystems) on a 7500 Fast Real-Time PCR system (Applied Biosystems).

***PhPDR2* cloning strategy:** Partial sequences of putative ABCG/*PDR* transcripts were amplified from total cDNA of W115 individuals. NBD1-specific amplicons of around 0.5 kb were obtained with 5’-mgwatgactctdytkytkggacctcc targeting PDR signature 1 and 5’-gyttcytytgncchcchgaaatwcc targeting the ABC signature. NBD2-specific amplicons of around 0.5 kb were obtained with 5’-gggwaaracggwgtyagtggwgcw targeting the Walker A box and 5’-ctcatnacaatdgcwgcwgctctwgc targeting PDR signature 3. Fragments for the respective NBDs were aligned and the *ABCG/PDR* subfamily specific consensus primers (F 5’-tattgggacttgaaatttgtgccgatac, R 5’-gctccactaacacccatcagagctgtc) were designed to amplify putative *ABCG/PDR* coding regions spanning NBD1 and NBD2 from W115 trichome cDNA.

Amplification of upstream and downstream sequences of *PhPDR2* full length transcript was achieved via 5’RACE and 3’RACE PCRs using the SMART-RACE cDNA Amplification Kit (Clontech, Takara Bio Company, USA) according to the manufacturers specifications. 5’ RACE primer and 5’ nested RACE primer had the following sequence: 5'-atggattcgaagaaggccagaacgtcttc and 5'-cccttaccatgtcatctcccaccaaag. 3’ RACE primer and nested 3’ RACE primer sequences were: 5'-gatcagggtgcctctgaagatagattgg and 5'-caggaggatatattgagggtagaatccaca.

The *PhPDR2* genomic DNA sequence was cloned in two sequential steps from W115 DNA. First, a 2.6 kb 5’ part was amplified (F 5’-atcccgggataatggaaccagtaaac, R 5’-ttaaggatccggatcccgtcatgtgaccaa, F contains a *Xma*I site and R a endogenous *Bam*HI

site (underlined)). The PCR product was T/A cloned into pGEM®-T easy (Promega). Second, the 3' 5.3 kb part of *PhPDR2* was amplified in to single PCRs. PCR1: F1 5'-ttaaggatccttggtcacatgacgggatcc with the endogenous *Bam*HI site (underlined), R1 5'-catcatcggtgaagtccagt. PCR2: F2 5'-gaagaaatggtggat, R2 5'-taagcggccgcctatcttgtctggaagtt with a *Not*I site (underlined). A second PCR (F1 and R2) resulted in amplification of the full 5.3 kb. The PCR product was cloned into pGEM®-T easy (Promega). Both genomic fragments were transferred into the binary pGreenII0229 vector system (Hellens et al. 2000). A *CaMV 35S* promoter was added with 5'-gggcccgtcaaagattcaaatagaggac and 5'-ctcgagtgtcctctccaaatgaaatg containing an *Apa*I and *Xho*I restriction site, respectively (underlined), a N-terminal *GFP5* was added with 5'-gtcgacatgagtaaaggagaagaac and 5'-ctgcagatctttcgaaagggcagatt containing a *Sal*I and *Pst*I restriction site, respectively (underlined), and an *OCE3* terminator was added with 5'-agcggccgcaatttccccgatcgttca and 5'-gcggccgccgatctagtaacatagatga containing *Not*I restriction sites (underlined).

***PhPDR2* promoter GUS constructs and GUS staining assay:** Amplification of a 1.2 kb promoter fragment upstream of the *PhPDR2* gene was accomplished via use of the Genome Walker Universal Kit (Clontech, Takara Bio Company, USA) with the primer 5'-caagagctgcccatttaagtgcttcttc and the nested primer 5'-cgcttaaacttccccttgcacttcctc. The fragment was T/A cloned into pGEM-T Easy vector system (Promega, USA) and subsequently reamplified with the primer 5'-ggaaccaagctttgtgtaggaaaattttgc containing a *Hind*III restriction site (underlined) and the primer 5'-tacatctagagacccccctctagctcag containing an *Xba*I restriction site (underlined). The respective restriction sites were used to clone the *PhPDR2* promoter fragment into the *GUS* gene-containing pGPTV-Bar (Becker et al. 1992) vector system.

For GUS staining trials tissues to be investigated were submerged in an appropriate amount of GUS-staining buffer (100 mM sodium phosphate buffer pH 7.0, 10 mM NaEDTA, 1.5 mM potassium hexacyanoferrate(II) trihydrate, 0.25 mM potassium hexacyanoferrate(III), 0.1% (v/v) Triton X-100 and 1 mM 5-bromo-4-chloro-3-indolyl β-D-glucuronide cyclohexylammonium salt) vacuum infiltrated three times for 30 s and incubated in the dark at 37 °C for 12 – 24 h. After staining samples were cleared and stored in 70% ethanol.

***PhPDR2* RNA interference constructs:** Silencing of *PhPDR2* specific transcripts was attempted via the generation of double stranded hairpin RNA fragments utilizing the pKANIBAL vector system (Wesley et al. 2001). A 407 bp fragment containing parts of the 3' end and the 3' UTR of *PhPDR2* was amplified from *PhPDR2* cDNA with 5'-cgatggatcctcgagctgatgatgaaacagtggaa, containing *BamH*I and *Xho*I restriction sites (underlined) and 5'-cgatatcgatggtaccgaataaatatgccgctttca containing *Cla*I and *Kpn*I sites (underlined). The resulting amplicon was cloned in sense and antisense direction in the two MCS of pKANIBAL flanking the hairpin intron sequence. The pKANIBAL RNAi cassette containing *CaMV 35S* promoter RNAi construct and *OCE3* terminator was excised from the vector backbone using the *Not*I restriction sites and transferred into the binary pGreenII0229 vector system (Hellens et al. 2000), conferring Glufosinate Ammonium resistance as a selection marker in plants.

After stable transformation of W115 plants the degree of down-regulation in several independent *PhPDR2* lines was estimated via semi-quantitative RT-PCR using the *PhPDR2* specific primers 5'-ggaatgtattctgccttacc and 5'-gtaatctccaaattgtgatgc. petunia tubulin 1 transcript, partially amplified with 5'-cattggtcaagccggttattc and 5'-acccttgaagaccagtacagt served as a housekeeping and loading control.

241 **Transient *Arabidopsis thaliana* transformation:** *Arabidopsis thaliana* Col-0 plants
242 were grown in a 8 h light, 16 h dark cycle at 21 °C at 60% relative humidity. Leaves of 2-
243 month-old plants were collected, the abaxial cuticule removed with sand paper, and
244 digested at 23 °C, gentle shaking, for 1.5 h in 0.4 M mannitol, 20 mM KCl, 20 mM MES,
245 0.4% [w/v] macerozyme R10 (Yakult Honsha, Japan), 1% [w/v] cellulase R10 (Yakult
246 Honsha, Japan), pH 5.7. After the digestion, 10 mM $CaCl_2$ was added, and protoplasts
247 were collected at 400 g for 5 min at 4 °C with low break. Supernatant was removed and
248 the pellet was solubilized in W5 solution (154 mM NaCl, 125 mM $CaCl_2$, 5 mM KCl, 2
249 mM MES, pH 5.7) was moved to a tube containing 21% [w/v] sucrose. The protoplasts
250 were collected at 400 g for 6 min at 4 °C with low break, the supernatant removed, and
251 cells were transferred to a new tube. W5 solution was added, the protoplasts were
252 incubated 30 min on ice, and collected at 400 g for 3 min at 4 °C with low break.
253 Protoplasts were collected and density was adjusted to $2 * 10^5$ cells ml^{-1} in MMg solution
254 (0.4 M mannitol, 15 mM $MgCl_2$, 4 mM MES pH 5.7).
255 The pGreen179 plasmid containing the 35S:GFP-PDR2 construct was purified with the
256 Plasmid Plus Midi Kit (Qiagen); 10 µg of the construct and 10 µg of the plasma
257 membrane marker *AtAHA2-RFP* (Lee et al. 2003) was added to the protoplasts, as well
258 as 220 µl of PEG solution (40% [w/v] PEG 4000, 0.2 M mannitol, 0.1 M $CaCl_2$).
259 Protoplasts were incubated for 5 min at 23 °C. Further, 800 µl of W5 solution was
260 added, and cells were collected 400 g for 3 min at 4 °C with low break. The supernatant
261 was removed fully, and 100 µl of W5 solution was added. Protoplasts were incubated in
262 the dark for 2 d at 23 °C.
263 **Stable petunia transformation:** *PhPDR2* promoter GUS constructs and *PhPDR2* RNAi
264 constructs were transferred into the W115 background via *Agrobacterium tumefaciens*

mediated transformation of leaf explants, callus induction and plant regeneration (Lutke 2006). 0.45% phytagel were used instead of 0.9% agar in all media and the concentrations of BAP and NAA in the Selection Medium was adjusted between 1 - 2 mg L^{-1} for the former and 0.05 - 0.15 mg L^{-1} for the latter to maximize shoot induction for each individual transformation.

Regenerated plantlets were tested for successful construct insertion via PCR on genomic DNA. The primers 5'-acggtccacatgccggtatatacgatg and 5'-gatggcatttgtaggagccaccttcc, targeting the *CaMV 35S* promoter, were used to confirm RNAi construct insertion. The primers 5'-gaattgatcagcgttggtgggaaagc and 5'-ggtaatgcgaggtacggtaggagttg, targeting the GUS gene, were used to confirm GUS construct insertion.

Trichome quantification: Leaves of 3-month-old, greenhouse-grown W115 plants (n=6) were quantified for trichome density. 0.5 cm^2 leaf fragments were collected at the middle leaf margin and on the middle leaf lamina. Each leaf fragment was then cut into five 0.5 x 0.1 cm strips for trichome quantification on both adaxial and abaxial sides at the stereomicroscope.

Sclareol growth assays: For the germination assay, seeds of wild type and *PhPDR2*-RNAi lines were grown on 0.5 MS – Suc plates supplemented with 0, 100, 250, or 500 µM sclareol. The germination rate was determined after xx days. For the root growth assay, wild type and *PhPDR2*-RNAi lines were grown on 0.5 MS – Suc plates for xx days, after which the plantlets were transferred to 0.5 MS – Suc plates supplemented with 0, 100, 250, or 500 µM sclareol. Primary root length was determined for plants grown on sclareol containing plates after xx days and expressed relative to plants grown

288 on plates not supplemented with sclareol. *PhPDR2* promoter GUS reporter containing
289 lines were grown and stained as described above.
290 ***Spodoptera littoralis* feeding trials:** All larvae for the leaf feeding experiments were
291 kindly provided by Syngenta, Switzerland. Second instar *S. littoralis* larvae were placed
292 in ventilated transparent plastic containers (10 * 10.5 * 4.5 cm). The bottom was covered
293 with a moist paper towel and every 1 - 2 days larvae were supplied with fresh leaves. It
294 was taken care, that their position and developmental stage were the same. The
295 uppermost fully expanded leaves were taken for feeding trials. To ensure that excised
296 leaves kept their turgor, cut petioles ends were inserted into small water containers and
297 sealed with parafilm. All larvae were weighted in regular intervals and their mortality was
298 recorded. A linear model using generalized least squares of the nlme package for the R
299 software (R Development Core Team, 2009, version 2.9.2) was utilized for comparing
300 weight of larvae at different time points. W115 data was set as intercept of the model.
301 Survival probabilities were calculated as Kaplan-Meier curves.
302 **Leaf washes:** Leaves of seven 3-month-old, greenhouse-grown W115, *pdr2*[1], *phdr2*[2],
303 and *pdr2*[3] plants were incubated with the adaxial surface in a glass petri dish with 8 ml
304 of isopropanol:acetonitrile:water 3:3:2 solution for 5 min at 23 °C with gentle shaking.
305 The solution was collected and stored at -20 °C for further use. Samples were
306 concentrated using Oasis HLB 6cc extraction cartridges (Waters). The cartridges were
307 conditioned with methanol, equilibrated with water, and loaded with the samples. After
308 washing with 5 ml water, the cartridges were eluted with 6 ml methanol. Samples were
309 dried under N_2, and resuspended in 200 µl of a isopropanol:acetonitrile:water solution
310 (Kang et al. 2010a) containing two internal standards, 0.05% (+) camphor-10-sulfonic
311 acid (purum, Fluka, Germany) and 0.05% lidocaine hydrochloride monohydrate (Sigma,

Germany). Samples were suspended in an ultrasonic bath for 1 min, centrifuged at 13'000 g at 4 °C for 5 min. 5 µl of the supernatant, were used for ultra-high performance liquid chromatography (UHPLC) coupled with high-resolution mass spectrometry (HR-MS).

UHPLC-HR-ESI-MS and MS/MS analyses: Samples were analyzed with an ultra-high performance (UHPLC) high-resolution mass spectrometry (HR-MS), which was composed of a Waters Acquity UPLC system (Waters, USA) connected to a maXis quadrupole time-of-flight MS (Bruker Daltonics, Germany). Plant metabolites were separated at 40 °C on a Waters Acquity UPLC BEH column (1 x 50 mm, 1.7 µm) with a flow rate of 0.2 ml min^{-1}, and a mobile phase composed of water (solution A) and acetonitrile (solution B), both of which containing 0.1% HCOOH. The gradient program conditions were: 3% of solvent B during 0.5 min followed by a linear gradient up to 99.5% within 8 min. The gradient was followed by a washing step with 99.5% solvent B for 2.5 min and a re-equilibration step to the initial composition for 2 min. The UHPLC was connected to the MS equipped with an electrospray ion source (ESI) operated either in positive (+) or in negative (-) ionization mode. Nitrogen was used as nebulizer (2.0 bar) and as dry gas (9 L min^{-1}, 205 °C) and as collision gas. MS acquisitions were performed in the mass range from *m/z* 50 to 1500 at 20'000 resolution (full width at half maximum) and 1.5 scan s^{-1}. Masses were calibrated below 2 ppm accuracy with a 2 mM solution of sodium formate over *m/z* 158 up to 1450 mass range prior analysis. MS/MS data consisted of averaged spectra acquired at 15, 20, and 30 eV collision energy, at 4 Hz scan rate, in the mass range *m/z* 50 to 800, and with N_2 as collision gas. Relative metabolite amounts were obtained by manual integration of corresponding signals found in theoretical extracted ion chromatograms (EIC) with ± 0.05 Da width.

336 The Bruker ProfileAnalysis™ application (Version 2.1, Bruker Daltonics, Germany) was
337 used for unsupervised principal component analysis (PCA) processing of the
338 HR-ESI-MS data. Conspicuous masses having more than 50% reduction of signal
339 intensity in *PhPDR2* lines compared to W115 were selected. The corresponding
340 molecular formulas of these masses were calculated at 2 ppm mass accuracy with
341 Smart Formula®, part of the DataAnalysis™ processing software (Bruker Daltonics,
342 Germany). Metabolites of interest for *Petunia sp.* were finally identified with SciFinder®
343 database (www.cas.org, American Chemical Society) and literature data (Elliger et al.
344 1988b; Elliger et al. 1988a; Elliger et al. 1989a; Elliger et al. 1990b; Elliger et al. 1990a;
345 Elliger and Waiss 1991; Elliger et al. 1992; Elliger et al. 1993; Tarling et al. 2013).
346 The UHPLC-HR-ESI-MS data was in addition processed with XCMS Online
347 (http://metlin.scripps.edu/xcms/, Metlin ((Tautenhahn et al. 2012) analyzing all *pdr2* lines
348 versus W115. Following parameters were selected: centwave detection method, 10 ppm
349 mass accuracy, 5 < UHPLC peak width < 20, obiwarp retention time correction, unpaired
350 parametric t-test (Welch t-test, unequal variances), 0.001 statistical threshold. Masses of
351 the aforementioned petuniasterols and petuniolides were identified in the XCMS results
352 file. The flavonoids were detected in negative ionization mode.
353 **Relative petuniolide and petuniasterone amounts in leaves:** Leaf margin (ca. 3 mm
354 from the edge) and inner side of the leaves were collected by cutting 3-month-old W115
355 plants (6 replicates) and two *pdr2*^{1}, *phdr2*^{2}, and *pdr2*^{3} plants each, and stored at –80°C
356 before extraction.
357 The leaves were immerged in liquid air, grinded manually at temperatures below –10°C.
358 To 50 mg of the frozen sample, 1 mL of the precooled (–18°C) extraction mixture 1
359 (methanol containing 2 µg mL^{-1} corticosterone (ISTD) / methyl tert-butyl methylether

(MTBE) 1:4) were added, shaken, incubated 10 min on ice, and sonicated for 10 min at 0°C. Then, 500 µL of extraction mixture 2 (water / methanol 3:1) was added at 23˚C. Following vortexing and centrifugation (2 min, 13'000 g), aliquots of the upper phases (600 µl) were transferred to new tubes and the solvent was evaporated with N_2 gas at 23˚C. Finally, the samples were re-suspended in 200 µL of acetonitrile / Isopropanol 7:3 and used for UHPLC-MS analysis.

Samples (1 µL injection) were analyzed with UHPLC-HR-MS instrumentation described above in a random sequence. Chromatographic conditions were different: Separation at 60°C on a Waters Acquity UPLC BEH C8 column (2.1 x 100 mm, 1.7 µm) with a flow rate of 0.4 ml min^{-1}, and a mobile phase composed of water (solution A) and acetonitrile (solution B), both them containing 1% of 1 M aq. NH_4OAc and 0.1% AcOH. Elution was started with 5% of solvent B during 1 min followed by a linear gradient up to 100% within 12 min. The gradient was followed by a washing step with 100% solvent B for 5 min and a re-equilibration step to the initial composition for 4 min. Data were quantitatively processed with the *Bruker Data Analysis* software by manual integration of the high-resolution extracted ion chromatograms (width of ± 0.01 Da) corresponding to the calculated exact masses of the following detected ionized molecules (EIC of the ionized species were combined to improve sensitivity) (Supplemental table 3).

The peak areas shown in figure 7 were normalized to 50 mg leaf material and to the ISTD according to following equation:

$$Area_{corr}[AU] = area_{compound} \times \frac{mass_{leaf}}{50\,mg} \times \frac{average(areas_{ISTD})}{area_{ISTD}}$$

Statistical analyses: Data were analyzed using the R software (R Development Core Team 2009), version 2.9.2. For comparing the weight (resp. weight gain) of larvae on

wildtype versus *pdr2* plants, a linear model using generalized least squares (gls) was applied from the package *nlme.* W115 data were set to represent the intercept of the model, against which each line is compared. From survival data, Kaplan-Meier estimates were calculated using the *survival* package in R, and *pdr2* survival curves were then tested for significant differences compared to the W115 curve. For all statistical analyzes, significance was reported at the level $\alpha = 0.05$.

Accession Numbers

Sequence data from this article can be found in the GenBank data library, the tomato genome database (http://mips.helmholtz-muenchen.de/plant/tomato/database), and the potato genome of Solgenomics network (http://solgenomics.net/organism/Solanum_tuberosum/genome) in under the following accession numbers:

Arabidopsis thaliana: At-*PDR1/ABCG29/*At3g16340 (BK001001), At-*PDR2/ABCG30/*At4g15230 (BK001000), At-*PDR3/ABCG31/*At2g29940 (BK001002), At-*PDR4/ABCG32/*At2g26910 (BK001003), At-*PDR5/ABCG33*/At2g37280 (BK001004), At-*PDR6/ABCG34/*At2g36380 (BK001005), At-*PDR7/ABCG35/*At1g15210 (BK001006), At-*PDR8/ABCG36/*At1g59870 (BK001007), At-*PDR9/ABCG37/*At3g53480 (BK001008), At-*PDR10/ABCG38/*At3g30842 (BK001009), At-*PDR11/ABCG39* /At1g66950(BK001010), At-*PDR12/ABCG40/*At1g15520 (BK001011), At-*PDR13/ABCG41/*At4g15215 (BK001012), At-*PDR14/ABCG42/*At4g15233 (BK001013), At-*PDR15/ABCG43/*At4g15236 (BK001014)

Glycine max: Gm-*PDR12* (Q1M2R7)

Nicotiana plumbaginifolia: Np-*PDR1* (AJ404328.1), Np-*PDR2* (AJ831424.1), Np-*PDR3* (AJ831379.1), Np-*PDR5* (JQ808000.1)

Nicotiana tabacum: Nt-*PDR1* (AB075550.1), Nt-*PDR3* (AJ831379.1), Nt-*PDR4* (AJ831380.1), Nt-*PDR5a* (JQ808002.1), Nt-*PDR5b* (JQ808003.1)

Oryza sativa: Os-*PDR1* (BK001015), Os-*PDR2* (BK001016), Os-*PDR3* (BK001017), Os-*PDR4* (BK001018), Os-*PDR5* (AJ535050), Os-*PDR6* (AJ535049), Os-*PDR7* (AJ535048), Os-*PDR8* (AJ535047), Os-*PDR9* (AJ535046), Os-*PDR10* (AJ535045), Os-*PDR11* (AJ535044), Os-*PDR12* (AJ535043), Os-*PDR13* (AJ535042), Os-*PDR15* (AJ535041), Os-*PDR16* (AAQ01165.1), Os-*PDR17* (AK100858), Os-*PDR18* (AK072827), Os-*PDR20* (EAZ44307.1), Os-*PDR21* (AK070409), Os-*PDR22* (AK107869), Os-*PDR23*_1 (AK102367), Os-*PDR23*_2 (AK103110)

Petunia hybrida: Ph-*PDR1* (JQ292813), Ph-*PDR2* (KU665392)

Solanum lycopersicum: Solyc02g081870.2.1, Solyc06g076930.1.1, Solyc05g018510.2.1, Solyc11g007300.1.1, Solyc06g036240.1.1, Solyc12g098210.1.1, Solyc09g091660.2.1, Solyc12g100190.1.1, Solyc12g100180.1.1, Solyc12g019640.1.1, Solyc11g067000.1.1, Solyc11g007290.1.1, Solyc11g007280.1.1, Solyc09g091670.2.1, Solyc08g067620.2.1, Solyc08g067610.2.1, Solyc06g065670.2.1, Solyc05g055330.2.1, Solyc05g053610.2.1, Solyc05g053600.2.1, Solyc05g053590.2.1, Solyc05g053570.2.1, Solyc03g120980.2.1

Solanum tuberosum: St-*PDR1* (JF720054.1), St-*PDR2* (JF440348.1), St-*PDR3* (JF720055.1), St-*PDR4* (JF720056.1) PGSC0003DMC400041247 PGSC0003DMT400061280, PGSC0003DMC400051611 PGSC0003DMT400076208, PGSC0003DMC400023214 PGSC0003DMT400034124, PGSC0003DMC400051609 PGSC0003DMT400076206, PGSC0003DMC400023219 PGSC0003DMT400034130,

PGSC0003DMC400051612 PGSC0003DMT400076209, PGSC0003DMC400033296 PGSC0003DMT400049313, PGSC0003DMC400033294 PGSC0003DMT400049311, PGSC0003DMC400029466 PGSC0003DMT400043433, PGSC0003DMC400033295 PGSC0003DMT400049312, PGSC0003DMC400004038 PGSC0003DMT400005783, PGSC0003DMC400004040 PGSC0003DMT400005785, PGSC0003DMC400032813: 1-1200 PGSC0003DMT400048449, PGSC0003DMC400050377 PGSC0003DMT400074382, PGSC0003DMC400050376.

Spirodela polyrrhiza: *Sp-TUR2* (CAA94437)

Results

Screen for *PDR* sequences expressed in leaves and trichomes

To identify petunia secondary metabolite transporters possibly involved in herbivore defense, a screen for PDR transcripts present in leaves and trichomes was performed with degenerate consensus primers targeting a highly conserved region of Solanaceae PDR sequences. Thirty-two cloned and sequenced amplicons of 0.5 kilobase (kb) size could be assigned to four putative genes, *PhPDR2* - *PhPDR5* (Figure 1). The *PhPDR2* fragment was the most abundant comprising 47% of the analyzed sequences. *PhPDR3* comprised 25% of the amplified sequences, whereas *PDR4* and *PDR5* were lowest in abundance comprising 16% and 12% the sequences, respectively. *PhPDR2* was amplified from trichomes as well as from leaves devoid of trichomes. *PhPDR4* was mainly expressed in trichomes, while *PhPDR3* and *PhPDR5* were mainly found in leaf tissue (Supplemental Figure 1).

A phylogenetic analysis was performed to relate petunia *PhPDR2* – *PhPDR5* fragments to reported PDR sequences of petunia, tomato (*Solanum lycopersicum*), rice (*Oryza sativa*), Arabidopsis (*Arabidopsis thaliana*), *Nicotiana sp*., *Spirodela polyrrhiza*, and soybean (*Glycine max)* (Supplemental Figure 2). This analysis assigned *PhPDR2*, *PhPDR3*, and *PhPDR4* to cluster I of PDR proteins and *PhPDR5* to cluster III (Supplemental Figure 2)(Crouzet et al. 2006). An additional phylogenetic analysis with focus on functionally characterized PDR genes (Xi et al. 2011; Sasabe et al. 2002; van den Brule and Smart 2002; Jasinski et al. 2001; Lee et al. 2005; Ducos et al. 2005; Galbiati et al. 2008; Chen et al. 2011; Bienert et al. 2012; Eichhorn et al. 2006; Kobae et al. 2006; Ito and Gray 2006; Campbell et al. 2003; Bessire et al. 2011; Trombik et al.

2008; Badri et al. 2008; Kim et al. 2007; Kretzschmar et al. 2012), revealed that all petunia *PDR* fragments, except *PhPDR2*, clustered closely with already characterized *PDR* sequences (Figure 1). PhPDR3 was found to be highly homologous with NpPDR1, while the trichome-specific PhPDR4 was near identical with NtPDR1. Closest relatives of PhPDR2 were NtPDR1, NpPDR1, AtPDR12, and GmPDR12 (Supplemental Figure 2), with an amino acid identity of 81%, 80%, 69%, and 65%, respectively. Because of the distinctiveness of PhPDR2 and its relatively high abundance we decided to focus further investigations on this sequence. To avoid possible redundancy PhPDR3 and PhPDR4 were dismissed from further analyses as they were likely orthologous with well-characterized NpPDR1 (Jasinki et al. 2001, Stukkens et al. 2005) and NtPDR1 (Sasabe et al. 2002, Couzet et al. 2013) respectively.

The 7541 bp genomic DNA sequence (start ATG to stop TGA) of *PhPDR2* consisted of 20 exons (Supplemental Figure 3A). 265 bp upstream of the start ATG, a putative methyl jasmonate (MJA)-responsive element (AACGTG) (Guerineau et al. 2003), was detected. Sequencing of the full length *PhPDR2* cDNA revealed an ORF of 4287 base pairs (bp), an 5' UTR of 135 bp, 3`UTR of 253 bp followed by a poly-A tail, resulting in a cDNA size of 4701 bp. The predicted polypeptide of 1429 amino acid residues and a molecular mass of ~162 kD featured a reverse organization of the two NBDs and the transmembrane domains (TMDs), distinct for full size ABCG type transporters (Supplemental Figure 3B). The *PhPDR2* NBDs contain the ATP-binding Walker A and B motifs (Walker et al. 1982), the ABC signatures (Martinoia et al. 2002), and all four PDR signatures (van den Brule and Smart 2002).

***PhPDR2* subcellular localization and expression pattern**

PDR proteins characterized to date localized exclusively to the plasma membrane. For localization of PhPDR2, its genomic sequence was fused to a green fluorescent protein (GFP) reporter sequence (*P35S:GFP-gPDR2*). *At-AHA2*, fused to a red fluorescent protein (*P35S:cAHA2-RFP*), served as a marker for plasma membrane localization (Lee et al. 2003). *Arabidopsis thaliana* mesophyll protoplasts were transiently co-transformed with the aforementioned constructs, and fluorescent signals were recorded. The overlay of the GFP and RFP signals revealed co-localization of the two recombinant proteins (Figure 2), indicating that PhPDR2 localized to the plasma membrane.

To investigate whether *PhPDR2* was expressed in tissues other than trichomes and leaves, quantitative RT-PCR was performed on RNA extracted from 14-day-old seedlings, from two-month-old roots and stems, from flower tissue and from selected leaf regions, and the values were expressed relative to expression in full leaf samples. *PhPDR2* transcripts were detected in low amounts in flowers, to a higher degree in whole seedlings, roots and stems, and in highest amounts in leaf samples (Figure 3A). *PhPDR2* expression was higher in leaf borders than in the central part of the leaf. Leaves devoid of trichomes showed lower expression of *PhPDR2* than full leaf samples, and transcription of *PhPDR2* was significantly enriched in pure leaf trichome samples (Figure 3A).

In order to obtain a more detailed picture of *PhPDR2* expression on a tissue specific level, a 1.2 kb genomic fragment upstream of the *PhPDR2* coding sequence was fused with the GUS reporter gene and stably transformed into the petunia cultivar W115. In foliar tissue, *PhPDR2* promoter activity was found around the leaf margins (Figure A) and in multicellular glandular trichomes (Figure 4B-C), including the epidermal cells

basal to the trichomes (Figure 4C). In stem tissue, expression was likewise restricted to trichomes (Figure 4D). Belowground, promoter activity was pronounced in and around developing and emerging lateral root primordia (Figure 4E), *PhPDR2* transcripts were also detected in flower tissue, particularly the stigma (Figure 4F).

To determine elements regulating *PhPDR2* expression, its transcriptional response to various biotic and abiotic stress treatments was monitored. Pathogens commonly elicit a salicylic acid (SA) dependent response, whereas herbivores elicit a jasmonic acid (JA) dependent response (Smith et al. 2009). Thus, the response of *PhPDR2* to SA and JA was investigated. In addition, the response to yeast extract, serving as a general fungal elicitor, was tested. To examine putative implications of *PhPDR2* in abiotic stress responses, we analyzed its transcript levels in response to abscisic acid (ABA), a phytohormone involved in water stress, the auxin analogue 1-naphtaleneacetic acid (NAA), the osmotic stress inducer mannitol, and sodium chloride, causing salt stress (Figure 3B). *PhPDR2* transcripts accumulated markedly in seedling roots and shoots treated with MJA, suggesting an involvement in herbivore defense. However, in mature plants, this induction was not observed anymore (Supplemental Figure 4 D-G). NtPDR5, previously reported to be involved in herbivore defense, was reported to be induced similarly upon JA treatment, but also upon mechanical wounding or application of oral secretion of *Manduca sexta* larvae, a Solanaceae specialist (Bienert et al. 2012). The transcriptional response of *PhPDR2* to the aforementioned treatments was investigated and it was found that *PhPDR2* is not responsive to mechanical wounding or to the application of *M. sexta* oral secretion (Supplemental Figure 4E-G).

pdr2 lines are less toxic to caterpillars

For functional analysis of *PhPDR2*, *Petunia hybrida* W115 plants were transformed with a *PhPDR2*-RNAi construct. The three *PhPDR2*-RNAi lines *pdr2*^{1}, *pdr2*^{2}, and *pdr2*^{3}, displaying high to moderate *PhPDR2* transcript silencing, were chosen for further analysis (Figure 5A). To test the hypothesis that PhPDR2 is involved in herbivore defense, caterpillars of the generalist herbivore *Spodoptera littoralis* were fed on *pdr2* leaves and on the respective wild-type leaves. Larval mortality and larval weight were monitored for larvae initially displaying the same average weight. Larval mortality rates were lower for larvae feeding on *pdr2* lines at all examined time points (Figure 5B) and from day 9 until day 13 of feeding, significantly higher average weight was measured for larvae feeding on *pdr2* leaves as compared to such feeding on wild-type leaves (Figure 5C). For example on day 13, chances of survival were nine times higher on *pdr2* than on wild-type leaves, and larval weight was 3.8 fold higher.

Decreased metabolite contents in *pdr2* lines

PDR proteins related to *PhPDR2* have been shown to be involved in sclareol transport (Jasinski et al. 2001; Kang et al. 2011). *PhPDR2*, however, did not show a transcriptional response to sclareol and *pdr2* lines did not show an increased susceptibility to sclareol as compared to wild-type (Supplemental Figure 5), making implications of PhPDR2 in sclareol transport unlikely.

Instead of testing of additional single substrates, we decided to undertake an untargeted metabolomics profiling for PhPDR2 substrate identification. Briefly, *pdr2* and wild-type leaves were incubated in an organic solvent mixture, concentrated, and analyzed using ultra-high performance liquid chromatography coupled with high-resolution mass spectrometry (UHPLC-HR-MS). Unsupervised principal component analysis revealed

fifteen conspicuous candidate masses with MS signal intensities lower than 50% in two or more *pdr2* lines compared to the wild type. In order to improve the tracking of reduced metabolites, a two-group processing with the XCMS platform (see methods) was used and included feature detection, retention time correction, alignment, annotation and statistical analysis (Tautenhahn et al. 2012). Data obtained revealed 57 features with fold ≤ 0.66, P-values ≤ 0.01, and intensities ≥ 1,000. Grouping the features, considering their accurate masses, and generating chemical formulae allowed the attribution of 28 of them to 11 petuniasterone and petuniolide derivatives (Table 1, Supplemental Table 1). The structures of the most abundant plant steroids were further confirmed by MS/MS in comparison with data obtained from reference petuniasterone A (Figure 6, Supplemental Figure 6). The compounds detected are present in several Petunia species, among them *Petunia hybrida* (Elliger et al. 1988a; Elliger et al. 1989a; Elliger et al. 1989b) and exhibit a strong insecticide activity. Furthermore, the XCMS processing revealed 29 features corresponding to 18 reduced metabolites that could not be identified so far (Supplemental Table 2).

To investigate whether the reduction of the steroidal compounds in *pdr2* lines was specific or if secondary metabolite levels in general were lower, we decided to further quantify a quercetin and a kaempferol galactopyranosides, two flavonoids that are well investigated in petunia (Zerback et al. 1989). Both were detected in similar amounts in *pdr2* and wild type, suggesting that the lower amounts of petuniasterones and petuniolides in *pdr2* lines were a specific effect (Table 1, Supplemental Table 1).

Finally, the relative concentrations of ca. 50 different plant steroids that have been characterized in several *Petunia* species, such as *P. hybrida, P. integrifolia, P. inflata, P. axillaris*, and *P. parodii* were estimated. Because some of them share the same

582 chemical formula, 37 extracted ion chromatograms (EICs) were calculated out of the
583 UHPLC-HR-ESI-MS data. This data processing allowed for the detection of 62.2% of
584 reported petuniasterone and petuniolide derivatives, whereof 65.2% were of lower
585 intensities in *pdr2* leaves compared to wild-type leaves (Supplemental Table 2).
586 To test whether differential petuniolide and petuniasterone contents between wild-type
587 and *pdr2* were reflected on the whole leaf level we performed UHPLC-HR-M-based
588 quantification on the inner leaf lamina and leaf margins. Leaf margins were assessed
589 separately since they showed a strong *PhPDR2*-Promoter GUS signal. Congruent with
590 findings for trichomes (Table 1), petuniolides A, C, E were highly abundant and were
591 found at significantly lower amounts in *pdr2* lines as compared to the wild-type ($p < 0.0005$). The less abundant petuniolides F1-4 were also significantly reduced in *pdr2* ($p < 0.0005$) compared to wild type samples, a trend also observed for petuniasterones A acetate, G1/G2, and I/P3 (Figure 7, Supplemental Figure 7). The two orders of magnitude difference in signal intensities between petuniolide E and petuniasterone H in whole leaf extracts were consistent with the findings for trichome extracts (Supplemental table 1). Interestingly, levels of the highest abundant petuniasterone, petuniasterone L/R, did not differ between *pdr2* and wild type samples, indicating an accumulation independent of PhPDR2 (Figure 7).
600 Petuniolide A was significantly more abundant in the marginal areas for both wild type ($p = 0.01$) and *pdr2* ($p = 0.006$), when compared to inner leaf lamina. For the other petuniolides, the differences between inner leaf lamina and leaf margin were not significant in the wild type, while they were significant in *pdr2* ($p < 0.01$). The different Petuniolid A distribution observed in leaf lamina and margins might be dependent on differences in trichome abundance or *PhPDR2* expression patterns, as *PhPDR2* is

606 expressed in both cell types. Therefore we quantified trichome density in leaf lamina and
607 margins, both on adaxial and abaxial sides. No significant differences in trichome
608 density were scored (521 +/- 95 adaxial lamina; 764 +/- 162 abaxial lamina; 850 +/- 142
609 adaxial margin; 925 +/- 147 abaxial margin; n=12. P value adaxial lamina to margin =
610 0.08; p value abaxial lamina to margin = 0.47). Therefore we suggest that *PhPDR2*
611 expression at the leaf borders is responsible for the higher accumulation of steroidal
612 compounds at the margins, compatible with PhPDR2 function against herbivore attacks.
613

Discussion

PhPDR2 is a PDR/ABCG protein expressed in glandular trichomes of leaves and stem

Toxic or deterrent secondary metabolites have been recognized as important means for herbivory defense (Schilmiller et al. 2008) and they are commonly found in high concentrations at exposed sites, such as the heads of glandular trichomes (Shroff et al. 2008; Weinhold and Baldwin 2011) and leaf margins (Schweizer et al. 2013). Postulating functional implications of primary active secondary metabolite transport to build up and maintain concentration gradients across membranes at glandular trichomes, we decided to screen for PDR transporters of petunia (Supplemental Figure 1) that are preferentially expressed in trichomes.

Four new petunia PDR sequences were identified and brought into phylogenetic context with characterized members of the PDR subclass (Figure 1), revealing the absence of close homologues for PhPDR2. PhPDR2 is a typical PDR/full-size ABCG protein featuring a reverse domain orientation (Supplemental Figure 3B) and localizing to the plasma membrane (Figure 2). Distinct expression of *PhPDR2* in leaf borders and trichomes was demonstrated by RT-PCR (Figure 4A) and GUS reporter studies (Figure 4). Congruence of both approaches suggest that the promoter region used correctly targets *PhPDR2* expression. *PhPDR2* is expressed in all stalk cells of the trichome (Figure 4 C-D). Collectively this data points towards a contribution of PhPDR2 in the export of substances from trichomes into the apoplastic space, possibly enhanced in proximity to the glandular head.

A role for *PhPDR2* in herbivory

638 To date, NtPDR5 is the only plant transporter reportedly involved in herbivore defense.
639 Similar to *pdr2*, *Ntpdr5* plants are more susceptible to herbivore feeding (Bienert et al.
640 2012). However, unlike *PhPDR2*, *NtPDR5* is induced in leaf tissue upon mechanical
641 wounding, application of *Manduca sexta* oral secretion or feeding (Supplemental Figure
642 4)(Bienert et al. 2012). The differences in expression of *PhPDR2* and *NtPDR5*, as well
643 as their distant phylogenetic relationship (Figure 1, Supplemental Figure 2), suggest
644 deviating roles in defense responses. The expression pattern of *PhPDR2* suggests an
645 involvement as a constitutive and unspecific component as a first line of defense in
646 trichomes and the leaf borders. Though upregulated by JA at the seedling stage,
647 PhPDR2 is unresponsive to chemical or mechanical feeding stimuli. *NtP*DR5 on the
648 other hand appears to be part of an inducible defense strategy that works locally at sites
649 of attack. Our results underline the importance of active transport of secondary
650 metabolites across trichome cells in plant defense against herbivores.
651
652 **Insecticidal petuniasterone and petuniolide contents are lower in *pdr2* lines**
653 A first attempt to identify potential substrates of PhPDR2 involved a targeted approach.
654 Close relatives of PhPDR2 have been implicated in terpenoid or sclareol transport
655 (Jasinski et al. 2001; van den Brule et al. 2002; Campbell et al. 2003; Crouzet et al.
656 2013). However, we could not observe a difference between wild-type and *pdr2* lines in
657 various sclareol assays (Supplemental Figure5). Metabolite contents of wild-type and
658 *pdr2* lines were analyzed with UHPLC-HR-MS and revealed the presence of several
659 secondary metabolites reduced in *pdr2* lines, among them many steroidal compounds
660 (Table 1, Supplemental Tables 1 and 2). The levels of two flavonoids remained
661 unchanged, corroborate the specificity of *pdr2* involvement in steroidal compound

662 transport (Table 1, Supplemental Table 1). The accurate masses and the resulting
663 chemical formulae of several candidates are corresponding to petuniasterones and
664 petuniolides, both steroidal compounds (Table 1, Supplemental Tables 1 and 2). MS/MS
665 confirmed their structures, in particular comparison of the fragmentation pattern of
666 extracted petuniasterone A acetate with petuniasterone A reference material
667 (Supplemental Figure 6).
668 Petuniasterones were first identified 1988 in petunia leaves (Elliger et al. 1988b; Elliger
669 et al. 1989a) within a screen for substances exhibiting toxicity to insect larvae. These
670 compounds contained a ketone moiety at the A-ring, and were therefore termed
671 petuniasterones (Supplemental Table 1). Later, the structure of a second class of
672 steroidal compounds with a spiro-lactone A-ring was described and called petuniolides
673 (Supplemental Table 1).
674 Petuniasterones with a linear side chain (*e.g.* petuniasterone H, Supplemental Figure 6)
675 are not toxic to insects, whereas orthoester derivatives (*e.g.* petuniasterone A) are toxic
676 against a wide variety of caterpillars, among them the *Solanaceae* specialist *Manduca*
677 *sexta*, or the *Spodoptera sp.* generalists (Elliger and Waiss 1991). In our experiments,
678 we find both, petuniasterones with linear and orthoester side chains to be present in
679 lower amounts in *pdr2* lines. Petuniolides typically have an orthoester side chain, and a
680 rearranged sterol backbone containing lactone ring. In general, petuniolides are about
681 10-fold more toxic than petuniasterones (Elliger and Waiss 1991). A possible mode of
682 action was proposed for petuniolides C and D, which were shown to be weak ligands of
683 rat brain GABA receptors (Isman et al. 1998). Cockroaches with a mutated GABA
684 receptor were less susceptible to various insecticides and displayed elevated resistance
685 against petuniolides (Isman et al. 1998).

686 We found several petuniolides and petuniasterones with high intensity to be significantly
687 reduced in *pdr2* lines (Table 1), irrespective of the sampling method (for trichomes, see
688 Table 1, for leaf lamina and leaf margins, see Figure 7 and Supplemental Figure 7).
689 Trichomes, major sites of *PhPDR2* expression (Figure 4B-D), are recognized to play an
690 important role in herbivore defense (Wang et al. 2001; Yazaki 2006; Schilmiller et al.
691 2008; Slocombe et al. 2008; Loreto et al. 2014). Leaf margins also express *PhPDR2*
692 (Figure 4A), and they were also reported to have insecticidal properties. In Arabidopsis,
693 specific accumulation of insecticidal glucosinolate in leaf margins has been reported
694 (Schweizer et al. 2013). The same report identified leaf margins as preferential feeding
695 sites of *S. littoralis* once the glucosinloate biosynthesis was impaired. Most of the
696 petuniolides and petuniasterones were indeed found to be more abundant in the leaf
697 margins as compared to the inner leaf lamina though in the wild type the differences
698 were significant only for petuniolide A (Figure 7, Supplemental Figure 7). The high
699 abundance of petuniolides A, C, and E in leaf margins might be implicated in warding off
700 generalists like *S. littoralis* that tend to prefer to feed on the margins if they are not
701 particularly protected. Thus the function of petuniolides in petunia would be similar to the
702 observed function of glucosinolate in leaf margins of Arabidopsis (Schweizer et al.
703 2013). Indeed, we found that *S. littoralis* feeding on *pdr2* leaves to gain weight faster
704 and to survive better than larvae feeding on wild type leaves (Figure 6). As both,
705 petuniasterone and petuniolide levels are reduced in *pdr2* lines; larvae feeding on *pdr2*
706 leaves ingest less toxic compounds per unit leaf material.
707 Petuniolide C was suggested to be the most relevant substance in *P. parodii* because of
708 its high toxicity and abundance (Elliger and Waiss 1991) (Dereeper et al. 2008). We also
709 identified petuniolide C in our samples, although in lower amounts than petuniolide A or

710 E (Supplemental Figure 7). Given their high abundance and toxicity and their high
711 decrease in *pdr2*, however, these three compounds are likely the main contributors to
712 the observed herbivory phenotype. The contrast to published data could be due to
713 different metabolite abundance in *P. hybrida*, or due to the slightly different growth
714 condition or extraction methods. Although most petuniasterones and petuniolides were
715 reduced in *pdr2* lines, not all levels were lover in *pdr2* lines (Supplemental Table 2,
716 Figure 7), which could indicate a specificity of PhPDR2 for selected molecules or
717 precursors. Also, not all reported petuniasterones and petuniolides were identified in our
718 experiments, and it should be kept in mind that besides masses corresponding to known
719 petuniasterones and petuniolides, around 18 further down-regulated components were
720 present in lower amounts in *pdr2* lines (Supplemental Table 2). The corresponding
721 chemical formulae have not been described for petunia so far and the structures could
722 not be elucidated with MS/MS experiments. Therefore we cannot exclude that some of
723 them may also be involved in PhPDR2-mediated herbivore resistance of petunia.
724 To address exact function of *PhPDR2* expression around emerging lateral roots and in
725 floral reproductive tissues (Figure 4 F-H) additional studies are needed. It is possible
726 that petuniolides are exuded in the rhizosphere to protect emerging later roots from
727 belowground herbivory, however in the case of the stigma, exudation of insecticidal
728 compounds would be highly detrimental for an insect-pollinated plant such as petunia.

729 Petuniasterones and petuniolides have a sterol backbone. Sterol transporters were first
730 identified in humans and yeast. Heterodimers of human ABCG5 and ABCG8 are
731 responsible for cholesterol and phytosterol export from the liver to the bile (Klett and
732 Patel 2003; Moitra et al. 2011; Tarling et al. 2013) and mutations in either cause
733 sitosterolemia, a disease characterized by the failure of cholesterol and phytosterol

734 excretion (Wittenburg and Carey 2002). About half of the 20 characterized ABC
735 members of humans are involved in transport of lipids or lipid-derived compounds, and
736 the proteins are either localized in the plasma membrane or in endosomal
737 compartments (Tarling et al. 2013). Similarly in yeast, ABCG proteins have been
738 reported to be involved in cholesterol, phytosterol, and ergosterol transport, the latter
739 being a structural sterol (Li 2004; Jungwirth and Kuchler 2006; Cabrito et al. 2011). In
740 *Arabidopsis thaliana*, ABCG9 and ABCG31 were very recently reported to be involved in
741 steryl-glycoside deposition in pollen (Choi et al. 2014). The finding that a large number
742 of ABCG-type ABC transporters is likely to act as sterol transporters supports the
743 hypothesis of PhPDR2 being a sterol transporter involved in the export of
744 petuniasterones and petuniolides. However, due to the fact that these compounds are
745 not commercially available we were unable to provide direct proof via transport assays.
746 A further obstacle in directly demonstrating transport activity is the hydrophobicity of
747 these compounds, which is the reason, why direct evidence was also not provided for
748 other Arabidopsis transporting lipidic compounds.
749 We conclude that *Petunia hybrida* PhPDR2 is a trichome and leaf-margin-localized
750 plasma-membrane intrinsic protein with a major role in herbivore defense against
751 generalist feeders. Considering demonstrated affinities of ABCG transporters for
752 steroidal compounds across kingdoms and the finding that downregulation of *PhPDR2* is
753 associated with reduced amounts of petuniasterones and petuniolides we postulate that
754 PhPDR2 is involved in the export of steroidal, insecticidal compounds.
755

Acknowledgements

We thank Christian Gübeli for technical support, and Prof. Ian Baldwin from the Max Planck Institute for Chemical Ecology in Jena, Germany for the supply of *Manduca sexta* oral secretion. This work was supported by the Swiss National Foundation within the NCCR Plant Survival.

GenBank accession number

BankIt1891159 PHPDR2 KU665392

Author contributions

E.M., J.S., L.Bi., and T.K. designed the research, J.S., M.S., M.L., L.Bo., G.W., L.Bi., and T.K. performed the research, J.G. and L.Bi contributed new analysis tools, J.S., L.Bi, E.M., and T.K. wrote the publication.

774 **References**

775

776 Badri DV, Loyola-Vargas VM, Broeckling CD, et al (2008) Altered profile of secondary
777 metabolites in the root exudates of Arabidopsis ATP-binding cassette transporter
778 mutants. Plant Physiol 146:762–771.

779 Banasiak J, Biala W, Staszkow A, et al (2013) A Medicago truncatula ABC transporter
780 belonging to subfamily G modulates the level of isoflavonoids. Journal of
781 Experimental Botany 64:1005–1015.

782 Becker D, Kemper E, Schell J, Masterson R (1992) New plant binary vectors with
783 selectable markers located proximal to the left T-DNA border. Plant Mol Biol
784 20:1195–1197.

785 Besser K, Harper A, Welsby N, et al (2009) Divergent regulation of terpenoid
786 metabolism in the trichomes of wild and cultivated tomato species. Plant Physiol
787 149:499–514.

788 Bessire M, Borel S, Fabre G, et al (2011) A Member of the PLEIOTROPIC DRUG
789 RESISTANCE Family of ATP Binding Cassette Transporters Is Required for the
790 Formation of a Functional Cuticle in Arabidopsis. Plant Cell 23:1958–1970.

791 Bienert MD, Siegmund SE, Drozak A, et al (2012) A pleiotropic drug resistance
792 transporter in Nicotiana tabacum is involved in defense against the herbivore
793 Manduca sexta. Plant J 72:745–757.

794 Bleeker PM, Mirabella R, Diergaarde PJ, et al (2012) Improved herbivore resistance in
795 cultivated tomato with the sesquiterpene biosynthetic pathway from a wild relative.

796 Proc Natl Acad Sci USA 109:20124–20129.

797 Bodenhausen N, Reymond P (2007) Signaling pathways controlling induced resistance
798 to insect herbivores in Arabidopsis. Mol Plant Microbe Interact 20:1406–1420.

799 Cabrito TR, Teixeira MC, Singh A, et al (2011) The yeast ABC transporter Pdr18 (ORF
800 YNR070w) controls plasma membrane sterol composition, playing a role in multidrug
801 resistance. Biochem J 440:195–202.

802 Campbell EJ, Schenk PM, Kazan K, et al (2003) Pathogen-responsive expression of a
803 putative ATP-binding cassette transporter gene conferring resistance to the
804 diterpenoid sclareol is regulated by multiple defense signaling pathways in
805 Arabidopsis. Plant Physiol 133:1272–1284.

806 Chen G, Komatsuda T, Ma JF, et al (2011) An ATP-binding cassette subfamily G full
807 transporter is essential for the retention of leaf water in both wild barley and rice.
808 Proc Natl Acad Sci USA 108:12354–12359.

809 Choi H, Ohyama K, Kim YY, et al (2014) The Role of Arabidopsis ABCG9 and ABCG31
810 ATP Binding Cassette Transporters in Pollen Fitness and the Deposition of Steryl
811 Glycosides on the Pollen Coat. Plant Cell 26:310–324.

812 Crouzet J, Roland J, Peeters E, et al (2013) NtPDR1, a plasma membrane ABC
813 transporter from Nicotiana tabacum, is involved in diterpene transport. Plant Mol
814 Biol. 82: 181-192

815 Crouzet J, Trombik T, Fraysse AS, Boutry M (2006) Organization and function of the
816 plant pleiotropic drug resistance ABC transporter family. FEBS Letters 580:1123–

817 1130.

818 Cutler HG, Reid WW, Delétang J (1977) Plant-Growth Inhibiting Properties of
819 Diterpenes From Tobacco. Plant Cell Physiol 18:711–714.

820 Dereeper A, Guignon V, Blanc G, et al (2008) Phylogeny.fr: robust phylogenetic analysis
821 for the non-specialist. Nucleic Acids Research 36:W465–W469.

822 Ducos E, Fraysse S, Boutry M (2005) NtPDR3, an iron-deficiency inducible ABC
823 transporter in Nicotiana tabacum. FEBS Letters 579:6791–6795.

824 Eichhorn H, Klinghammer M, Becht P, Tenhaken R (2006) Isolation of a novel ABC-
825 transporter gene from soybean induced by salicylic acid. J Exp Bot 57:2193–2201.

826 Elliger CA, Benson M, Haddon WF, et al (1989a) Petuniasterones. Part 2. Novel
827 ergostane-type steroids from Petunia hybrida vilm. (solanaceae). J Chem Soc,
828 Perkin Trans 1 143–149.

829 Elliger CA, Benson M, Lundin RE, Waiss ACJ (1988a) Minor Petuniasterones from
830 Petunia hybrida. Phytochemistry 27:3597–3603.

831 Elliger CA, Benson ME, Haddon WF, et al (1988b) Petuniasterones, Novel Ergostane-
832 Type Steroids of *Petunia hybridia* Vilm. (Solanaceae) Having Insect-Inhibitory
833 Activity. X-Ray Molecular Structure of the 22,24,25-[(Methoxycarbonyl)Orthoacetate]
834 of 7a,22,24,25-Tetrahydroxy Ergosta-1,4-Dien-3-One and of 1a-Acetoxy-24,25-
835 Epoxy-7a-Hydroxy-22-(Methylthiocarbonyl)Acetoxyergost-4-en-3-One. J Chem Soc,
836 Perkin Trans 1 711–717.

837 Elliger CA, Waiss AC Jr. (1991) Insect Resistance Factors in Petunia. In: ACS
838 Symposium Series. American Chemical Society, Washington, DC, pp 210–223

839 Elliger CA, Waiss AC, Benson M, Wong RY (1990a) Ergostanoids From *Petunia parodii*.
840 Phytochemistry 29:1–11.

841 Elliger CA, Waiss AC, Benson M, Wong RY (1993) Ergostanoids From *Petunia inflata*.
842 Phytochemistry 33:471–477.

843 Elliger CA, Waiss ACJ, Benson M (1992) Petuniasterone R, A New Ergostanoid From
844 Petunia parodii. Journal of Natural Products 55:129–133.

845 Elliger CA, Waiss ACJ, Wong RY, Benson M (1989b) Petuniasterones From Petunia
846 parodii And P. integrifolia; Unusual Ergostane-Type Steroids. Phytochemistry
847 28:3443–3452.

848 Elliger CA, Wong RY, Waiss AC, Benson M (1990b) Petuniolides. Unusual ergostanoid
849 lactones from Petunia species that inhibit insect development. J Chem Soc, Perkin
850 Trans 1 525.

851 Galbiati M, Simoni L, Pavesi G, et al (2008) Gene trap lines identify Arabidopsis genes
852 expressed in stomatal guard cells. Plant J 53:750–762.

853 Gerats T, Vandenbussche M (2005) A model system for comparative research: Petunia.
854 Trends in Plant Science 10:251–256.

855 Gershenzon J, Dudareva N (2007) The function of terpene natural products in the
856 natural world. Nat Chem Biol 3:408–414.

857 Guerineau F, Benjdia M, Zhou DX (2003) A jasmonate-responsive element within the *A.*
858 *thaliana* vsp1 promoter. Journal of Experimental Botany 54:1153–1162.

859 Hare JD (2005) Biological activity of acyl glucose esters from Datura wrightii glandular
860 trichomes against three native insect herbivores. J Chem Ecol 31:1475–1491.

861 Hellens RP, Edwards EA, Leyland NR, et al (2000) pGreen: a versatile and flexible
862 binary Ti vector for Agrobacterium-mediated plant transformation. Plant Mol Biol
863 42:819–832.

864 Howe GA, Jander G (2008) Plant immunity to insect herbivores. Annu Rev Plant Biol
865 59:41–66.

866 Hwang, J.U., Song, W-Y, Hong, D., Ko, D., Yamaoka, Y., Jang, S., Yim, S., Lee, E.,
867 Khare, D., Kim, K., Palmgren, M., Yoon, H.S., Martinoia, E. and Lee, Y. (2016) Plant
868 ABC transporters enable many unique aspects of a terrestrial plant's lifestyle. Mol. Plant
869 9, 338-355
870
871 Isman MB, Jeffs LB, Elliger CA, et al (1998) Petuniolides, Natural Insecticides from
872 *Petunia parodii,* Are Antagonists of $GABA_a$ Receptors. Pesticide Biochemistry and
873 Physiology 58:103–107.

874 Ito H, Gray WM (2006) A gain-of-function mutation in the Arabidopsis pleiotropic drug
875 resistance transporter PDR9 confers resistance to auxinic herbicides. Plant Physiol
876 142:63–74.

877 Jasinski M, Stukkens Y, Degand H, et al (2001) A plant plasma membrane ATP binding

878 cassette-type transporter is involved in antifungal terpenoid secretion. Plant Cell
879 13:1095–1107.

880 Jungwirth H, Kuchler K (2006) Yeast ABC transporters – A tale of sex, stress, drugs and
881 aging. FEBS Letters 580:1131–1138.

882 Kang J, Park J, Choi H, et al (2011) Plant ABC Transporters. Arabidopsis Book 9:e0153.

883 Kang JH, Liu G, Shi F, et al (2010a) The tomato odorless-2 mutant is defective in
884 trichome-based production of diverse specialized metabolites and broad-spectrum
885 resistance to insect herbivores. Plant Physiol 154:262–272.

886 Kang JH, Shi F, Jones AD, et al (2010b) Distortion of trichome morphology by the
887 hairless mutation of tomato affects leaf surface chemistry. J Exp Bot 61:1053–1064.

888 Kim D-Y, Bovet L, Maeshima M, et al (2007) The ABC transporter AtPDR8 is a cadmium
889 extrusion pump conferring heavy metal resistance. The Plant Journal 50:207–218.

890 Kim HK, Choi YH, Verpoorte R (2010) NMR-based metabolomic analysis of plants.
891 Nature Protocol 5:536-49

892 Klett EL, Patel S (2003) Genetic defenses against noncholesterol sterols. Curr Opin
893 Lipidol 14:341–345.

894 Kobae Y, Sekino T, Yoshioka H, et al (2006) Loss of AtPDR8, a plasma membrane ABC
895 transporter of Arabidopsis thaliana, causes hypersensitive cell death upon pathogen
896 infection. Plant Cell Physiol 47:309–318.

Kretzschmar T, Burla B, Lee Y, Martinoia E (2011) Functions of ABC transporters in plants. Essays Biochem. 50, 145-160

Kretzschmar T, Kohlen W, Sasse J, et al (2012) A petunia ABC protein controls strigolactone-dependent symbiotic signalling and branching. Nature 483:341–344.

Kreuz K, ToMMASINI R, Martinoia E (1996) Old Enzymes for a New Job (Herbicide Detoxification in Plants). Plant Physiol 111:349–353.

Lee J, Bae H, Jeong J, et al (2003) Functional expression of a bacterial heavy metal transporter in Arabidopsis enhances resistance to and decreases uptake of heavy metals. Plant Physiol. 133, 589-596

Lee M, Lee K, Lee J, et al (2005) AtPDR12 contributes to lead resistance in Arabidopsis. Plant Physiol 138:827–836.

Li Y (2004) ATP-binding Cassette (ABC) Transporters Mediate Nonvesicular, Raft-modulated Sterol Movement from the Plasma Membrane to the Endoplasmic Reticulum. Journal of Biological Chemistry 279:45226–45234.

Loreto F, Dicke M, Schnitzler J-P, Turlings TCJ (2014) Plant volatiles and the environment. Plant Cell Environ. 37:1905-1908.

Lutke WK (2006) Petunia (Petunia hybrida). Methods Mol Biol 344:339–349.

Martinoia E, Klein M, Geisler M, et al (2002) Multifunctionality of plant ABC transporters--more than just detoxifiers. Planta 214:345–355.

Moitra K, Silverton L, Limpert K, et al (2011) Moving out: from sterol transport to drug resistance – the ABCG subfamily of efflux pumps. Drug Metabolism and Drug Interactions. 26:105-111

Oerke EC (2005) Crop losses to pests. J Agric Sci 144:31.

Sasabe M, Toyoda K, Shiraishi T, et al (2002) cDNA cloning and characterization of tobacco ABC transporter: NtPDR1 is a novel elicitor-responsive gene. FEBS Letters 518:164–168.

Schaller H (2004) New aspects of sterol biosynthesis in growth and development of higher plants. Plant Physiology and Biochemistry 42:465–476.

Schilmiller AL, Last RL, Pichersky E (2008) Harnessing plant trichome biochemistry for the production of useful compounds. Plant J 54:702–711.

Schweitzer F, Fernández-Calvo P, Zander M (2013) Arabidopsis Basic Helix-Loop-Helix Transcription Factors MYC2, MYC3, and MYC4 Regulate Glucosinolate Biosynthesis, Insect Performance, and Feeding Behavior. Plant Cell, 25: 3117-3132

Shroff R, Vergara F, Muck A, et al (2008) Nonuniform distribution of glucosinolates in Arabidopsis thaliana leaves has important consequences for plant defense. Proc Natl Acad Sci USA 105:6196–6201.

Slocombe SP, Schauvinhold I, McQuinn RP, et al (2008) Transcriptomic and Reverse Genetic Analyses of Branched-Chain Fatty Acid and Acyl Sugar Production in *Solanum pennelli*i and *Nicotiana benthamiana*. Plant Physiol 148:1830–1846.

939 Smith JL, De Moraes CM, Mescher MC (2009) Jasmonate- and salicylate-mediated
940 plant defense responses to insect herbivores, pathogens and parasitic plants. Pest
941 Manag Sci 65:497–503.

942 Stukkens Y, Bultreys A, Grec S, et al (2005) NpPDR1, a pleiotropic drug resistance-type
943 ATP-binding cassette transporter from Nicotiana plumbaginifolia, plays a major role
944 in plant pathogen defense. Plant Physiol 139:341–352.

945 Tarling EJ, de Aguiar Vallim TQ, Edwards PA (2013) Role of ABC transporters in lipid
946 transport and human disease. Trends in Endocrinology & Metabolism 24:342–350.

947 Tautenhahn R, Patti GJ, Rinehart D, Siuzdak G (2012) XCMS Online: A Web-Based
948 Platform to Process Untargeted Metabolomic Data. Anal Chem 84:5035–5039.

949 Theodoulou FL (2000) Plant ABC transporters. Biochim Biophys Acta 1465:79–7103.

950 Tissier A, Sallaud C, Rontein D (2013) Tobacco Trichomes as a Platform for Terpenoid
951 Biosynthesis Engineering. In: Bach TJ, Rohmer M (eds) Isoprenoid Synthesis in
952 Plants and Microorganisms. Springer New York, pp 271–283

953 Trombik T, Jasinski M, Crouzet J, Boutry M (2008) Identification of a cluster IV
954 pleiotropic drug resistance transporter gene expressed in the style of Nicotiana
955 plumbaginifolia. Plant Mol Biol 66:165–175.

956 van Dam NM, Hare JD (1998) Biological activity of Datura wrightii glandular trichome
957 exudate against Manduca sexta larvae. J Chem Ecol 24:1529–1549.

958 van den Brule S, Muller A, Fleming AJ, Smart CC (2002) The ABC transporter SpTUR2

959 confers resistance to the antifungal diterpene sclareol. Plant J 30:649–662.

960 van den Brule S, Smart CC (2002) The plant PDR family of ABC transporters. Planta
961 216:95–9106.

962 Wagner GJ (1991) Secreting Glandular Trichomes: More than Just Hairs. Plant Physiol
963 96:675–679.

964 Wagner GJ, Wang E, Shepherd RW (2004) New approaches for studying and exploiting
965 an old protuberance, the plant trichome. Ann Bot 93:3–11.

966 Walker JE, Saraste M, Runswick MJ, Gay NJ (1982) Distantly related sequences in the
967 alpha- and beta-subunits of ATP synthase, myosin, kinases and other ATP-requiring
968 enzymes and a common nucleotide binding fold. EMBO J 1:945–951.

969 Wang EM, Wagner GJ (2003) Elucidation of the functions of genes central to diterpene
970 metabolism in tobacco trichomes using posttranscriptional gene silencing. Planta
971 216:686–691.

972 Wang EM, Wang R, DeParasis J, et al (2001) Suppression of a P450 hydroxylase gene
973 in plant trichome glands enhances natural-product-based aphid resistance. Nature
974 Biotechnology 19:371–374.

975 Weinhold A, Baldwin IT (2011) Trichome-derived O-acyl sugars are a first meal for
976 caterpillars that tags them for predation. Proc Natl Acad Sci USA 108:7855–7859.

977 Wesley SV, Helliwell CA, Smith NA, et al (2001) Construct design for efficient, effective
978 and high-throughput gene silencing in plants. Plant J 27:581–590.

979 Wittenburg H, Carey MC (2002) Biliary cholesterol secretion by the twinned sterol half-
980 transporters ABCG5 and ABCG8. J Clin Invest 110:605–609.

981 Xi J, Xu P, Xiang C-B (2011) Loss of AtPDR11, a plasma membrane-localized ABC
982 transporter, confers paraquat tolerance in Arabidopsis thaliana. The Plant Journal
983 69:782–791.

984 Yazaki K (2006) ABC transporters involved in the transport of plant secondary
985 metabolites. FEBS Letters 580:1183–1191.

986 Zerback R, Bokel M, Geiger H, Hess D (1989) A Kaempferol 3-Glucosylgalactoside and
987 further Flavonoids from Pollen of *Petunia hybrida*. Phytochemistry 28:897–899.

988

989

990

991

992

993

Figure legends

Figure 1. Phylogeny of Ph-*PDR* sequences

Phylogeny of *Petunia hybrida PDR2 – PDR5* fragments (blue) and the respective fragments, identified by sequence similarity, of reported PDR sequences of *Arabidopsis thaliana* (red), *Nicotiana tabacum* and *N. plumbaginifolia (*green), *Spirodela polyrrhiza* (black), rice (black), and *Glycine max* (black).

Figure 2. PDR2 localizes to the plasma membrane

Arabidopsis thaliana mesophyll protoplasts were transiently co-transformed with a 35S::*GFP-PDR2* construct and the plasma membrane marker AHA2-RFP. **(A)** PDR2 GFP signal, **(B)** AHA2 RFP signal, **(C)** overlay of **(A)** and **(B)**, **(D)**, bright field image of the same cell shown in **(A-C)**. Scale bar: 10 µm.

Figure 3. *PDR2* is expressed in leaf and stem trichomes and it is induced by jasmonic acid

(A) Quantitative PCR for *PDR2* in aboveground parts of 14-day-old seedlings and in different organs of a 2-month-old plant. Abbreviations: seedling (Seedl), flower (Flow), leaf margin (L mar) and leaf inner part (L inn), leaf devoid of trichomes (L – T), and trichomes (Trich). **(B)** Quantitative *PDR2* PCR in 24-day-old seedling root (light grey) and shoot (dark grew) treated with water, salicylic acid (SA), methyl jasmonate (MJA), abscisic acid (ABA), auxin (NAA), yeast extract (Yex), mannitol (Man), and sodium chloride (NaCl). **(A, B)** Data are depicted as means ± SE of three technical replicates of one representative biological sample.

Figure 4. Tissue-specific expression of *PDR2*

GUS expression of a two-month-old W115 *PDR2*::GUS in leaf **(A)**, in leaf trichomes **(B,C)**, in stem trichomes **(D)**, in the main root **(E)**, and in a flower **(F)**. Scale bars are 1 mm. No background staining was observed in plants not expressing GUS using the same conditions as for GUS expressing plants.

Figure 5. *Spodoptera littoralis* feeding on *pdr2* and wild type plants

(A) Quantitative PCR shows downregulation of PDR2 in *pdr2* lines compared to wild type. **(B, C)** *Spodoptera littoralis* second instar larvae feeding experiments over 16 days on 3-month-old *pdr2* lines 1-3 (grey bars and symbols) or on wild type (white bars and symbols). Depicted are weight gain over time (**B**, means ± SE, 30 biological replicates, $\alpha = 0.05$) or as survival rate over time **(C)**. The experiments shown are representatives for three experiments performed.

Figure 6. Petuniasterone MS/MS studies. MS/MS peaks and predicted corresponding fragment structures for Petuniolide E, a toxic steroidal compund found at lower concentrations in *pdr2* lines.

Figure 7. Relative petuniolide and petuniasterone levels in leaves and leaf margins of wild type and *pdr2* plants.

Petuniolide and petuniasterone amounts as detected by UHPLC HR-MS in wild type and *pdr2* leaf lamina and margins (wt lamina, white; pdr2 lamina, grey; wt margin, light grey; pdr2 margin, dark grey). Values are expressed as means ± SE, n = 6 (* $p < 0.05$; ** $p <$

1041 0.005; *** p < 0.0005). Values are normalized to wild type lamina levels. Absolute values

1042 are depicted in Supplemental Figure 7.

1043

1044

1045 Figure 1:

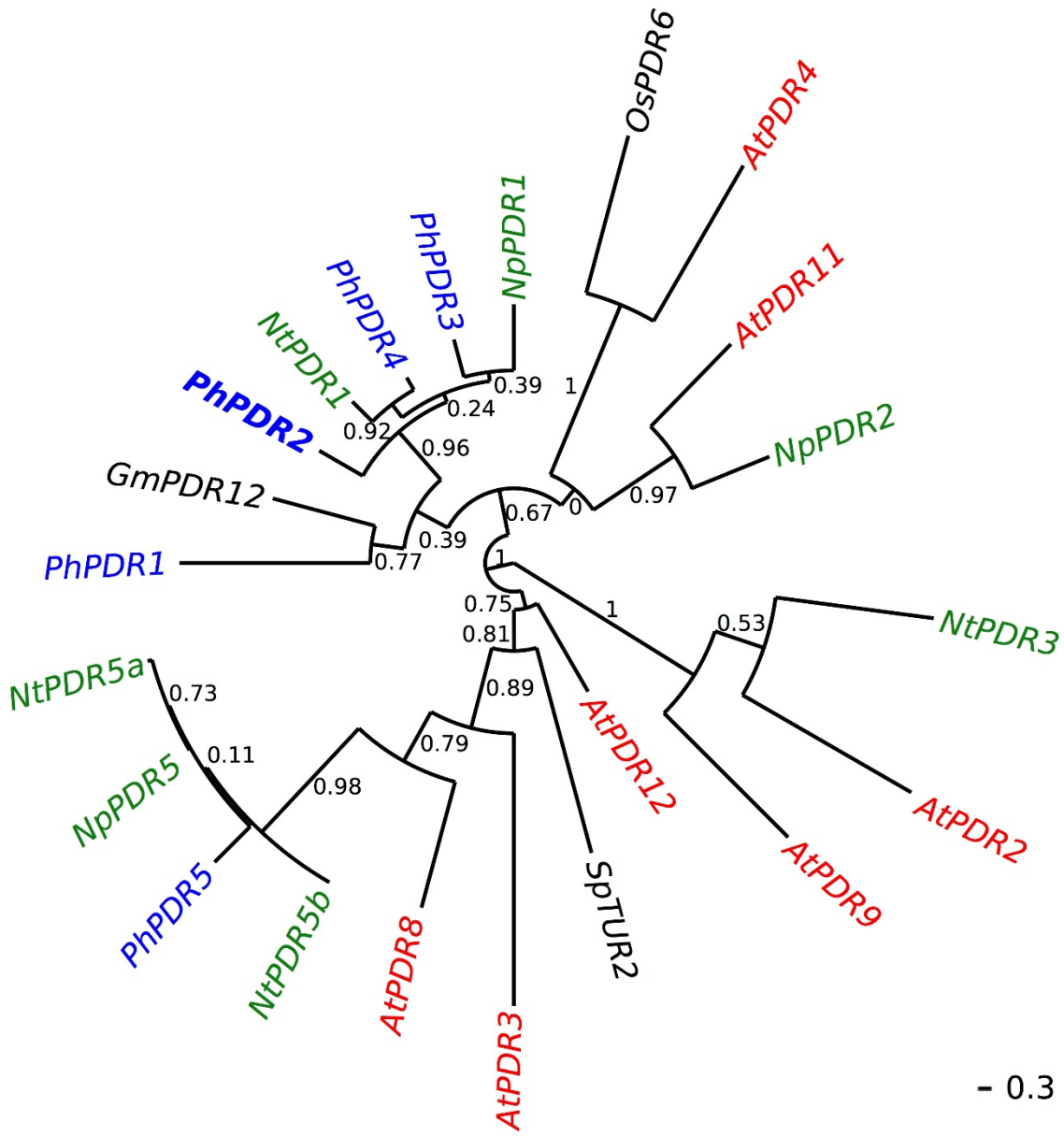

1046
1047

Figure 2:

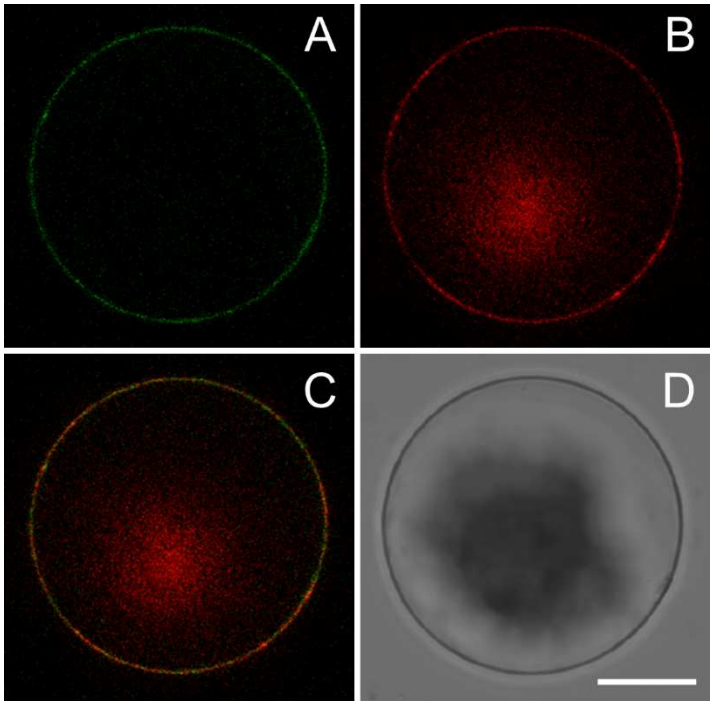

Figure 3:

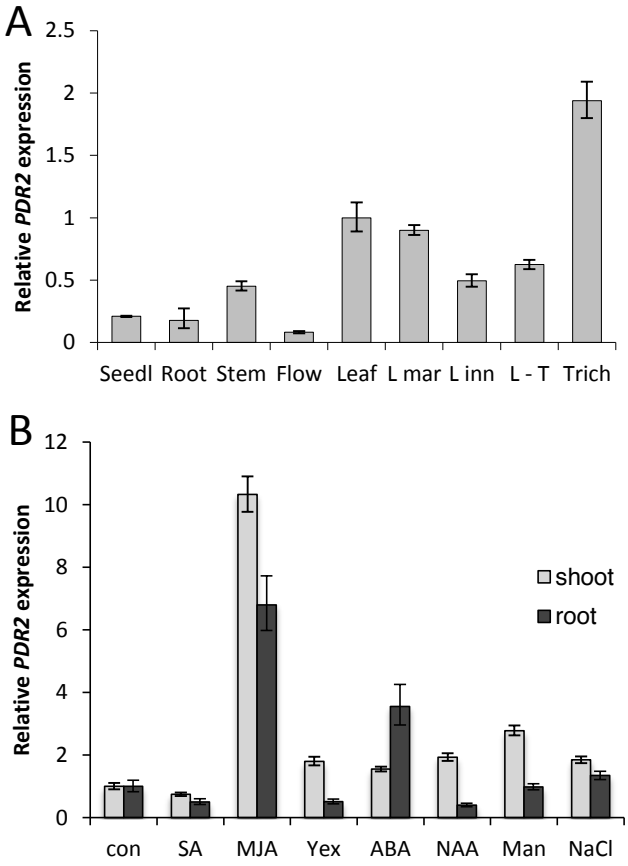
A
Relative PDR2 expression
2.5
2
1.5
1
0.5
0
Seedl
Root
Stem
Flow
Leaf
L mar
L inn
L - T
Trich
B
Relative PDR2 expression
12
10
8
6
4
2
0
shoot
root
con
SA
MJA
Yex
ABA
NAA
Man
NaCl

Figure 4:

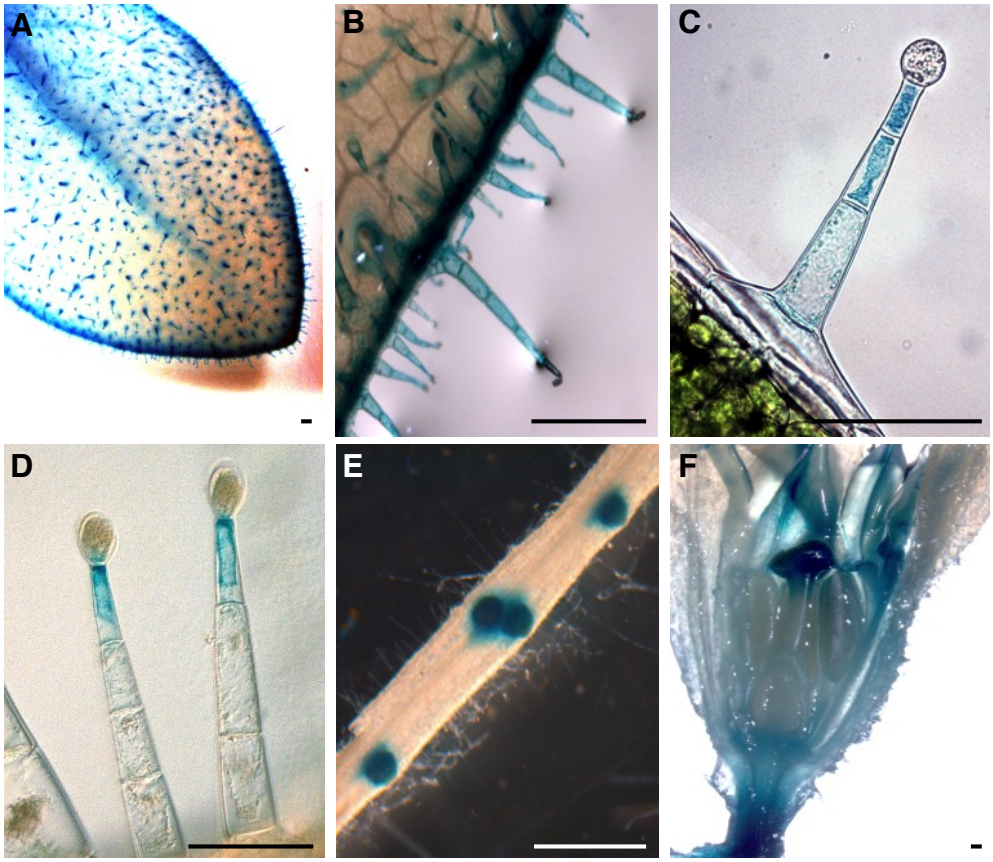

Figure 5:

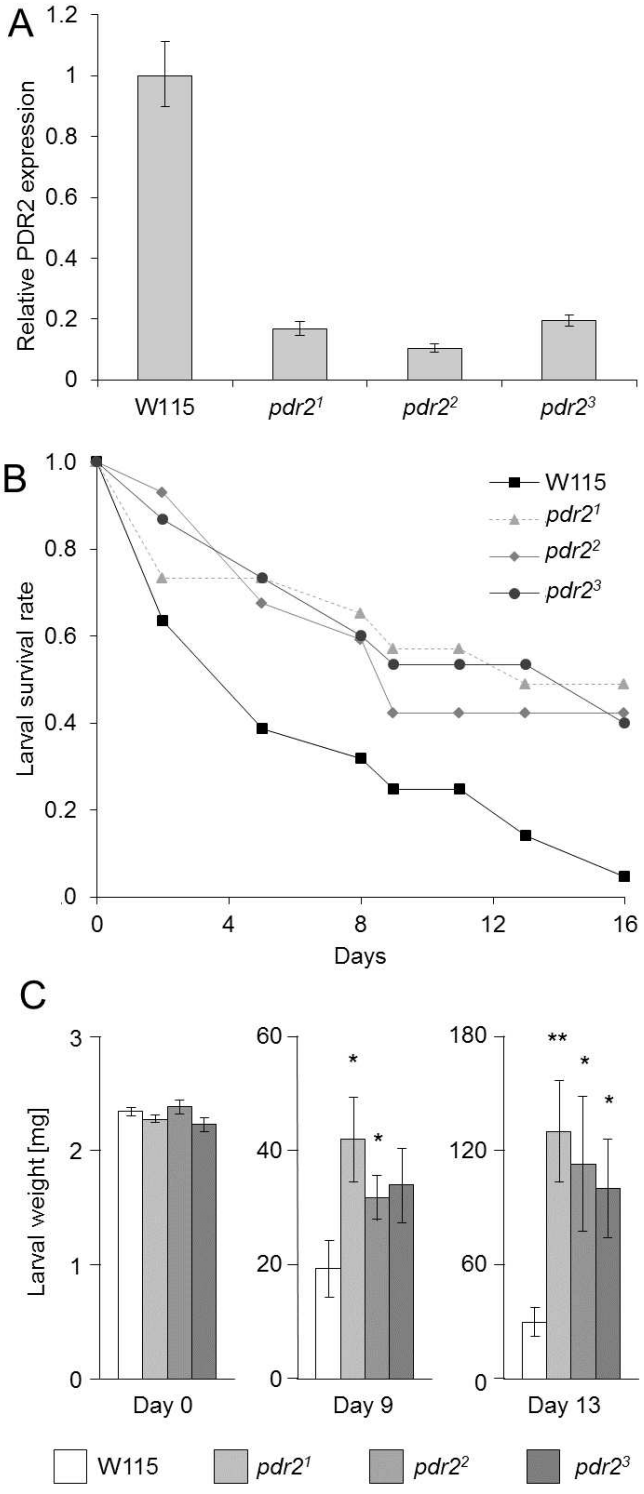
A
Relative PDR2 expression
1.2
1
0.8
0.6
0.4
0.2
0
W115
pdr2¹
pdr2²
pdr2³
B
Larval survival rate
1.0
0.8
0.6
0.4
0.2
0
0
4
8
12
16
Days
W115
pdr2¹
pdr2²
pdr2³
C
Larval weight [mg]
3
2
1
0
60
40
20
0
180
120
60
0
*
*
**
*
*
Day 0
Day 9
Day 13
W115
pdr2¹
pdr2²
pdr2³

Figure 6:

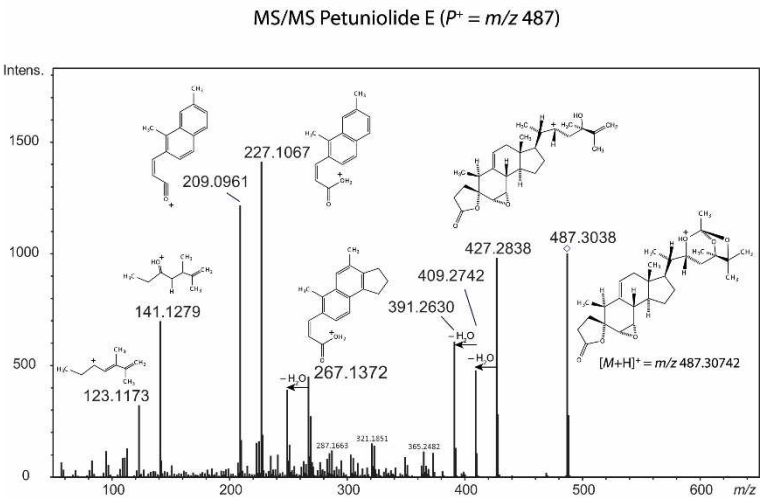
MS/MS Petuniolide E (P^+ = m/z 487)
Intens.
1500
1000
500
0
100
200
300
400
500
600
m/z
227.1067
209.0961
141.1279
123.1173
267.1372
391.2630
409.2742
427.2838
487.3038
$[M+H]^+$ = m/z 487.30742

Figure 7:

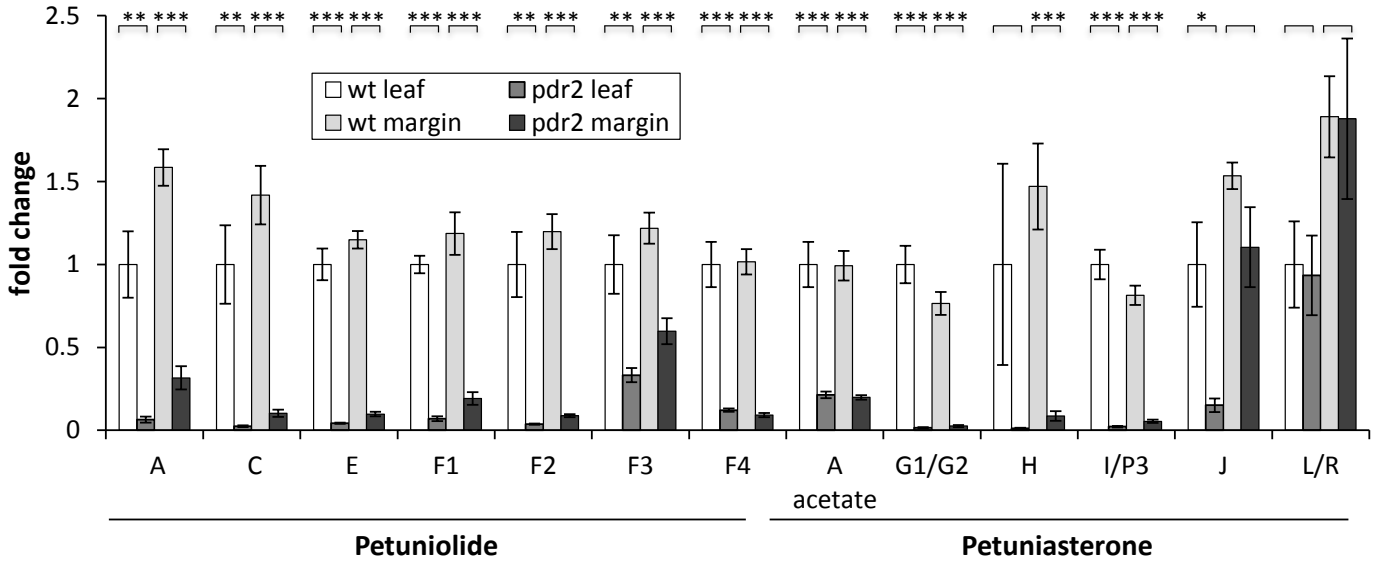
2.5
2
1.5
1
0.5
0
fold change
wt leaf
pdr2 leaf
wt margin
pdr2 margin
** *** ** *** ****** ****** ** *** ** *** ****** ****** ****** *** ****** * *
A C E F1 F2 F3 F4 A G1/G2 H I/P3 J L/R
acetate
Petuniolide
Petuniasterone

Supplemental Data:

Supplemental Methods

Additional *PDR2* induction experiments: For mechanical wounding and *M. sexta* oral secret treatment, *pPDR2-GUS* W115 plants (see below) were pre-selected by Basta spraying and grown on soil for 4 - 6 weeks. Plants were wounded at the youngest fully unfolded leaf by forceps pressure or by a fabric pattern wheel (Kallenbach et al. 2012). For oral secret treatment, 20 µl of secret (kindly provided by I. Baldwin, Max Planck Institute for Chemical Ecology, Jena, Germany), 33 mM MJA, or water was applied to the wounded parts of the leaf. After 24 h, plants were collected for GUS staining.

Sclareol phenotype assays: Three-week-old *PPDR2-GUS* plants grown on 0.5 MS + Suc plates were grown for further 24 h on 0.5 MS + Suc supplemented with 0, 100, or 500 µM sclareol to monitor if *PDR2* was sclareol responsive. Subsequently, plants were stained (see GUS staining).

Wild type and *PDR2* seeds were germinated on plates containing 0, 50, 250, or 500 µM sclareol and germination was scored after 11 days of growth (Campbell et al. 2003).

Wild type and *PDR2* plants were grown for two weeks on 0.5 MS – Suc, or on plates additionally supplemented with 30 mg L^{-1} Hygromycin, respectively. Subsequently, plants were transferred to 0.5 MS + Suc supplemented with 0, 100, 250, or 500 µM sclareol. Root length difference between day 0 and 6 on sclareol-containing plates was quantified and expressed as mean change of root length (Campbell et al. 2003).

Supplemental figure legends:

Supplemental Figure 1. *PDR* expression profile of petunia leaves and trichomes

PDR expression profile of petunia leaves and trichomes. Primers were designed to bind to the conserved Walker A and PDR signature 4 of second NBD. They were used to amplify fragments of PDR genes expressed in leaves and trichomes. A maximum likelihood tree is depicted for sequenced fragments, grouped according to similarity and

named in ascending numbers. The trichome or leaf symbol stands for the origin of the respective sequence.

Supplemental Figure 2. PhPDR phylogeny in comparison to other species

Maximum likelihood tree for 500 bp cDNA of PDR domains of *Petunia hybrida* (Ph, dark blue), *Oryza sativa* (Os, orange), *Arabidopsis thaliana* (At, red), *Nicotiana tabacum* (Nt, green), *Nicotiana plumbaginifolia* (Np, green), *Solanum lycopersicum* (Sl, light blue), *Spirodela polyrrhiza* (Sp, black), and *Glycine max* (Gm, black). Petunia sequences originate from amplification with primers aligning to Walker A domain and to PDR signature 4 on the second NBD. The same domain was identified in the sequences of non-Petunia species depicted by similarity search (Multalin tool). Probabilities are depicted as numbers at branching points. PDR clusters are annotated after Crouzet *et al*. 2005. Note that the fragment of *OsPDR1* is present in cluster IV rather than in cluster I described for the protein sequence. The *OsPDR14* pseudogene was excluded from the analysis, as well as *OsPDR23* and *OsPDR22* that did not contain the fragment of interest.

Supplemental Figure 3. Predicted structure of PDR2

(A) Genomic structure of PDR2, exons are depicted as boxes.

(B) PDR2 protein topology structure was predicted with ConPred II. Transmembrane domains (TMD) contain mainly hydrophobic (green circles) amino acids, whereas the nucleotide binding domains (NBD) contain additionally hydrophilic (blue), positive charged (red), and negatively charged (yellow) residues.

Supplemental Figure 4. Transcriptional responses of *PhPDR2*

A-C, Two-month-old, sterile-grown *pPDR2-GUS* plants were wounded (red squares) mechanically with a forceps (B) or a scissor (C). A, Negative control. (D), Relative *PhPDR2* expression in two-month-old, greenhouse-grown W115 plants. Control leaves were sampled at the day of treatment (1) and collection (2). One leaf of three plants each were wounded with a fabric pattern wheel with subsequent application of water (3-5), or 33 mM MJa (6-8), and collected after 24 h. E-G, one-month-old, sterile-grown *pPDR2-GUS* plants were wounded with a fabric pattern wheel with subsequent application of water (E), 33 mM methyl jasmonate (F), or *Manduca sexta* oral secret (G). A-C, E-G, plants were GUS-stained after 24 h of incubation.

Supplemental Figure 5. Sclareol assays

a) Seedlings of a pPDR2-GUS line were grown on different sclareol concentrations for 24 h and stained for GUS activity. b) W115 and PDR2-RNAi plants were grown on plates with and without sclareol. Difference in root length is depicted as mean ± s.e.m. N = 15. c) Seeds of W115 and PDR2-RNAi plants were grown for 11 d on different sclareol concentrations. Number of germinated (white, grey) and non-germinated (black) seeds are depicted.

Supplemental Figure 6. Petuniasterone MS/MS studies.

MS/MS peaks and predicted corresponding fragment structures for the reference compound Petuniasterone A, as well as the detected compunds Petuniasterone A acetate, Petuniasterone H and Petuniolide E.

Supplemental Figure 7. Absolute petuniolide and petuniasterone levels in leaves and leaf margins of wild type and *pdr2* plants.

Absolute peak intensities (AU, arbitrary units) of petuniolides and petuniasterones normalized by internal standard corticosterone and sample dry weight as detected by UHPLC HR-MS in wild type and *pdr2* leaf lamina and margins (wt lamina, white; pdr2 lamina, grey; wt margin, light grey; pdr2 margin, dark grey). Values are expressed as means ± SE, n = 6 (* $p < 0.05$; ** $p < 0.005$; *** $p < 0.0005$). Relative amounts are depicted in Figure 7.

Supplemental figure 1:

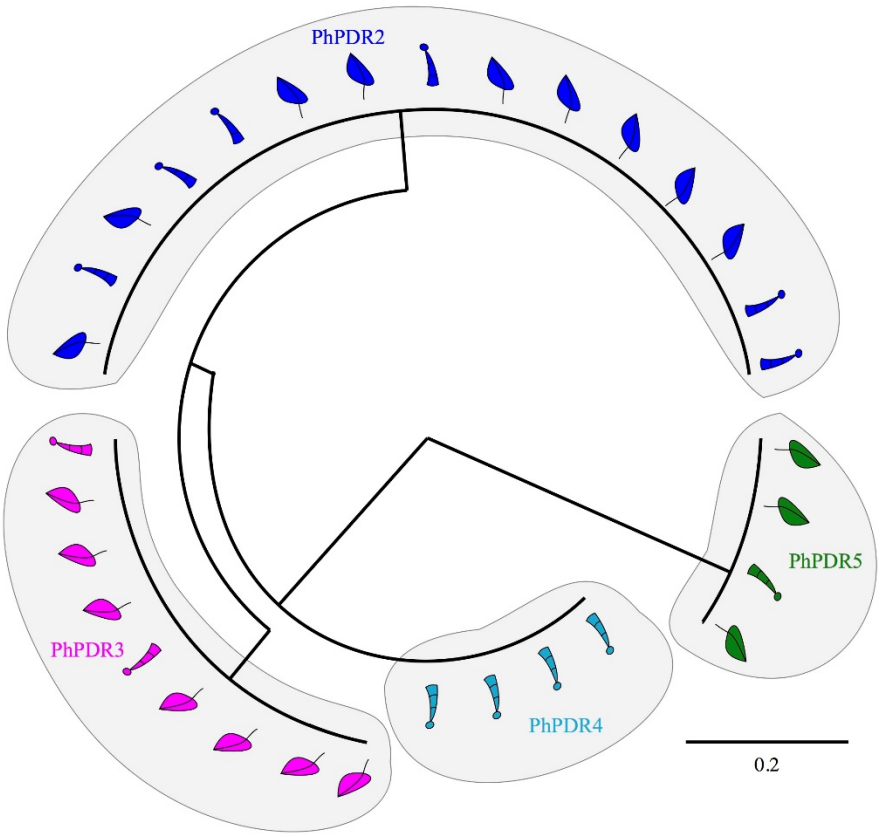

Supplemental figure 2:

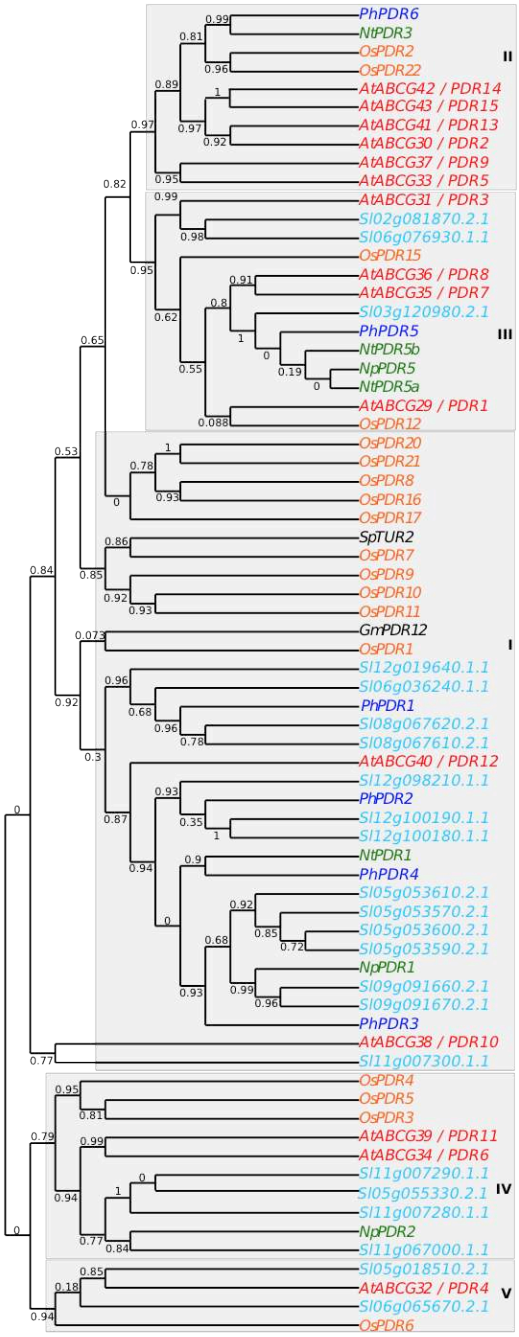

Supplemental figure 3:

A

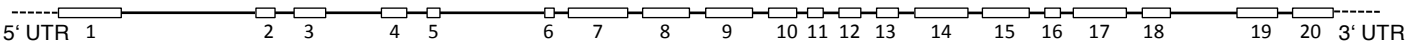

B

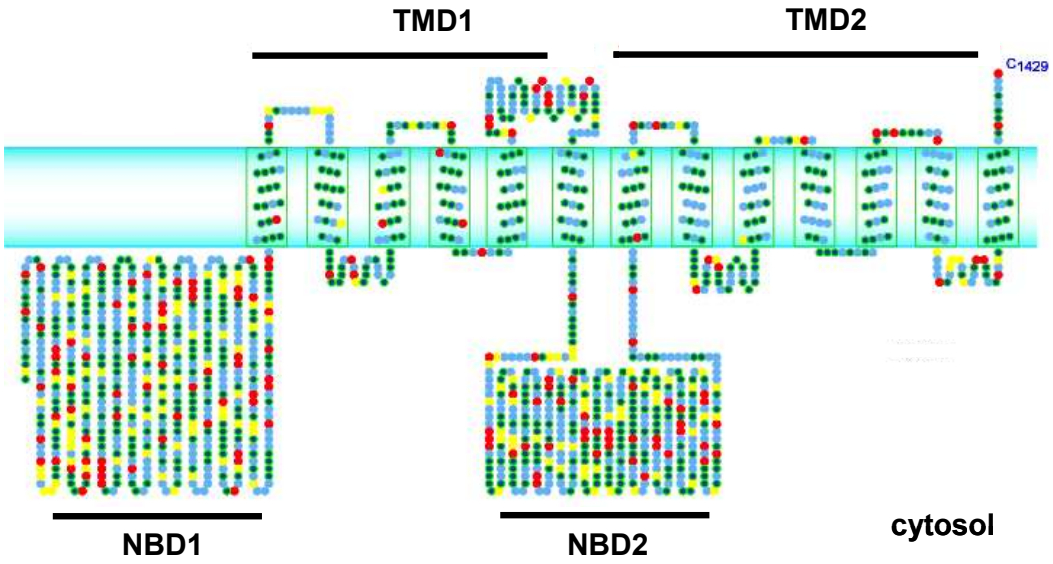

Supplemental figure 4:

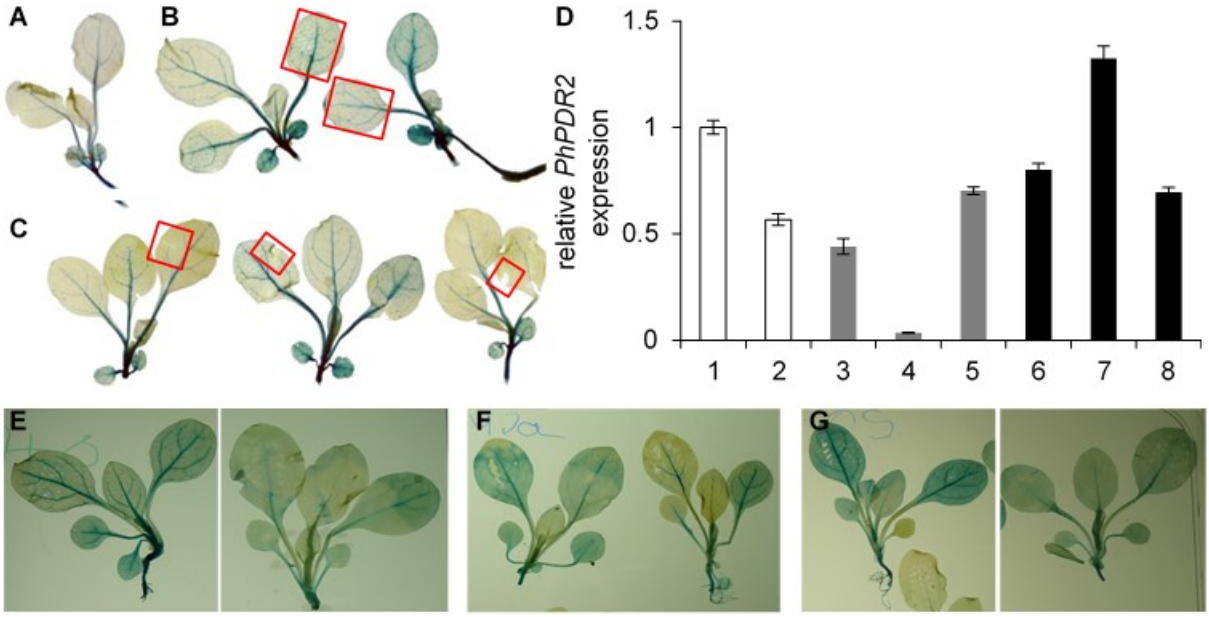

Supplemental figure 5:

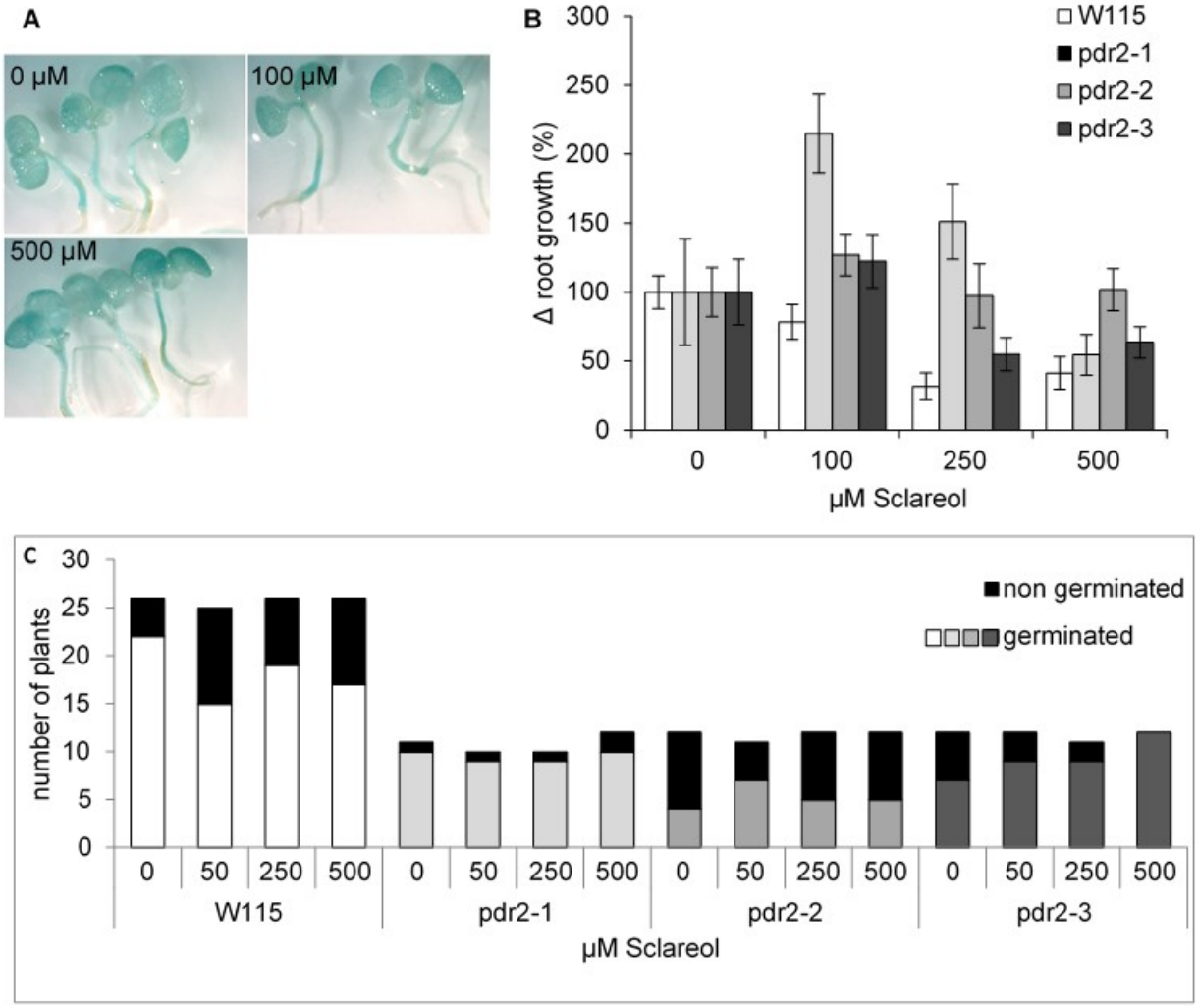

Supplemental figure 6:

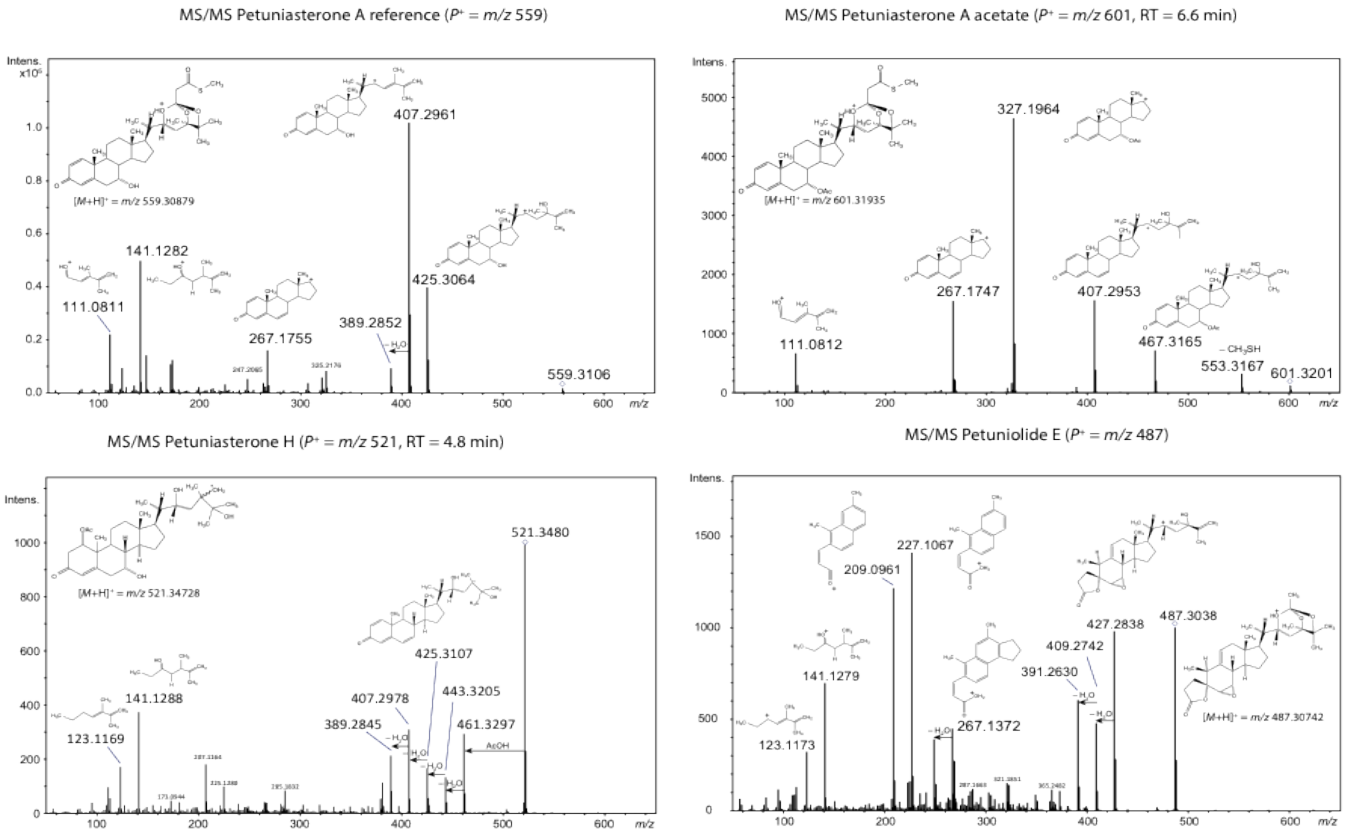

Supplemental figure 7:

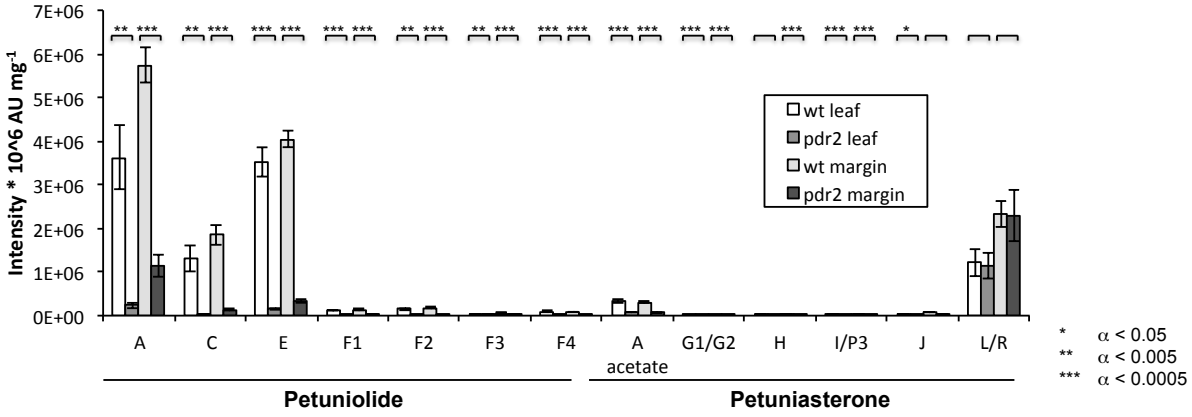

1228 Tables:

Table 1. Petuniasterone and petuniolide content reduction in pools of *pdr2* lines

Substance	Feature ID	Fold[1)]	p-value	m/z_{med}	m/z_{theo}	Accuracy [ppm]	Chemical Formula	Rt_{med} (min)	Intensity	Adduct / Fragment
Petuniolide E	#69	0.31	8.44E-04	391.2632	391.2632	**0.0**	$C_{27}H_{35}O_2$	**5.83**	3044	$[M+H-AcOH-2H_2O]^+$
	#55	0.31	4.76E-04	409.2742	409.2737	**-1.1**	$C_{27}H_{37}O_3$	**5.83**	2965	$[M+H-AcOH-H_2O]^+$
	#58	0.29	5.37E-04	427.2843	427.2843	**0.1**	$C_{27}H_{39}O_4$	**5.83**	15961	$[M+H-AcOH]^+$
	#39	0.29	2.95E-04	487.3044	487.3054	**2.1**	$C_{29}H_{43}O_6$	**5.83**	31407	$[M+H]^+$
	#28	0.22	1.59E-04	504.3325	504.3320	**-1.1**	$C_{29}H_{46}O_6N$	**5.83**	1028	$[M+NH_4]^+$
	#64	0.21	6.60E-04	509.2878	509.2874	**-0.8**	$C_{29}H_{42}O_6Na$	**5.83**	1180	$[M+Na]^+$
	#117	0.07	2.23E-03	990.6296	990.6301	**0.5**	$C_{58}H_{88}O_{12}N$	**5.83**	3572	$[2M+NH_4]^+$
	Avg:	**0.19**	**7.43E-04**	–	–	**–**	–	**–**	**59157**	= Σ intensities
Petuniolide A	#14	0.40	4.97E-05	425.2686	425.2686	**0.1**	$C_{27}H_{37}O_4$	**5.29**	25835	$[M+H-2AcOH]^+$
	#1	0.32	3.25E-07	485.2896	485.2898	**0.3**	$C_{29}H_{41}O_6$	**5.31**	5914	$[M+H-AcOH]^+$
	#4	0.32	3.17E-06	562.3345	562.3374	**5.3**	$C_{31}H_{48}O_8N$	**5.30**	2977	$[M+NH_4]^+$
	#2	0.29	3.99E-07	567.2923	567.2928	**0.9**	$C_{31}H_{44}O_8Na$	**5.30**	1374	$[M+Na]^+$
	Avg:	**0.33**	**1.34E-05**	–	–	–	–	–	**36100**	= Σ intensities
Petuniolide F3	#355	0.38	8.15E-03	503.3002	503.3003	**0.3**	$C_{29}H_{43}O_7$	**5.00**	9692	$[M+H]^+$
	#373	0.37	8.69E-03	443.2786	443.2792	**1.4**	$C_{27}H_{39}O_5$	**5.00**	6802	$[M+H-AcOH]^+$
	Avg:	**0.37**	**8.42E-03**	–	–	**–**	–	**–**	**16494**	: Σ intensities
Petuniasterone I/P3	#165	0.60	3.21E-03	633.3083	633.3092	**1.4**	$C_{34}H_{49}O_9S$	**5.46**	4601	$[M+H]^+$
	#244	0.63	5.54E-03	650.3341	650.3357	**2.6**	$C_{34}H_{52}O_9SN$	**5.46**	5587	$[M+NH_4]^+$
	#135	0.61	2.64E-03	655.2899	655.2911	**1.8**	$C_{34}H_{48}O_9SNa$	**5.46**	4079	$[M+Na]^+$
	Avg:	**0.61**	**3.80E-03**	–	–	**–**		**–**	**14267**	= Σ intensities
Petuniasterone G1/G2	#427	0.24	9.97E-03	407.2940	407.2945	**1.1**	$C_{28}H_{39}O_2$	**4.22**	1631	$[M+H-3H_2O]^+$
	#365	0.22	8.44E-03	425.3048	425.3050	**0.6**	$C_{28}H_{41}O_3$	**4.22**	3535	$[M+H-2H_2O]^+$
	#318	0.19	7.22E-03	443.3146	443.3156	**2.3**	$C_{28}H_{43}O_4$	**4.22**	6640	$[M+H-H_2O]^+$
	#335	0.18	8.24E-03	461.3301	461.3262	**-8.6**	$C_{28}H_{45}O_5$	**4.22**	2346	$[M+H]^+$
	Avg:	**0.20**	**8.47E-03**	–	–	**–**	–	**–**	**14152**	= Σ intensities
Petuniolide F2	#87	0.45	1.38E-03	503.3004	503.3003	**-0.1**	$C_{29}H_{43}O_7$	**4.70**	9201	$[M+H]^+$
	#122	0.45	2.33E-03	443.2785	443.2792	**1.6**	$C_{27}H_{39}O_5$	**4.70**	2670	$[M+H-AcOH]^+$
	Avg:	**0.45**	**1.86E-03**	–	–	**–**	–	**–**	**11871**	= Σ intensities
Petuniolide C	#416	**0.17**	**9.71E-03**	501.2851	501.2847	**-0.9**	$C_{29}H_{41}O_7$	**4.86**	**9891**	$[M+H]^+$
Petuniolide F1	#32	0.28	1.75E-04	503.3001	503.3003	**0.4**	$C_{29}H_{43}O_7$	**5.99**	6384	$[M+H]^+$
	#65	0.37	7.44E-04	443.2774	443.2792	**4.1**	$C_{27}H_{39}O_5$	**5.99**	3476	$[M+H-AcOH]^+$
	Avg:	**0.32**	**4.60E-04**	–	–	**–**	–	**–**	**9860**	= Σ intensities
Petuniasterone L/R	#33	0.40	1.99E-04	615.2970	615.2986	**2.6**	$C_{34}H_{47}O_8S$	**5.63**	4144	$[M+H]^+$
	#107	0.41	1.83E-03	615.2973	615.2986	**2.2**	$C_{34}H_{47}O_8S$	**5.25**	1671	$[M+H]^+$
	Avg:	**0.41**	**1.02E-03**	–	–	**–**	–	**–**	**5815**	= Σ intensities
Perulactone C/ D	#381	**0.19**	**8.94E-03**	535.3254	535.3265	**2.2**	$C_{30}H_{47}O_8$	**4.59**	**1577**	$[M+H]^+$
Petuniasterone H	#44	**0.20**	**3.35E-04**	521.3458	521.3473	**2.8**	$C_{30}H_{49}O_7$	**4.78**	1402	$[M+H]^+$
Q-3-GluGal	#3794[1)]	0.85	5.05E-01	625.1415	625.1410	**-0.8**	$C_{27}H_{29}O_{17}$	**2.20**	**16319**	$[M-H]^-$
K-3-GluGal	#4420	0.91	6.03E-01	609.1467	609.1461	**-1.0**	$C_{27}H_{29}O_{16}$	**2.35**	**9002**	$[M-H]^-$

Greenhouse-grown leaves were washed in buffer and metabolites were analyzed using the XCMS platform.
List of substances with the feature ID assigned by XCMS analysis, as well as the fold reduction and the p-value (data displayed is median of three *pdr2* lines), the measured mass (*m/z* med), the mass accuracy, retention time (RT med), and intensity. Chemical formula and accuracy were calculate with the SmartFormula software. For steroids with more than one feature, the average of the fold reduction, p-value and the sum of the intensities are given in addition. In addition to steroids, amounts of two flavonoids, Q-3-GluGal and K-3-GluGal (Quercetin 3-*O*-(2''-*O*-*β*-D-glucopyranosyl)-*β*-D-galactopyranoside and Kaempferol 3-*O*-(2''-*O*-*β*-D-glucopyranosyl)-*β*-D-galactopyranoside, respectively (Zerback et al. 1989)) were analyzed. Analysis of unknown metabolites can be found in Supplemental Table 2.

Supplemental tables:

Supplemental Table 1. Structure and amount of selected petuniasterone, petuniolide and flavonoid derivatives found in *pdr2* and wild-type lines

Compound and mass (*m/z*)	EIC	Box-Whisker Plot
Petuniasterone A acetate (601.3197, $[M+H]^+$)	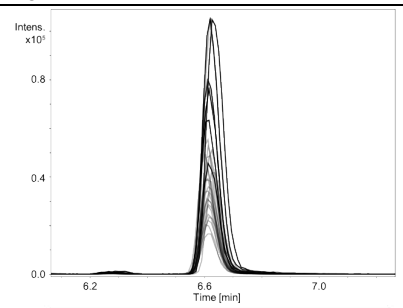	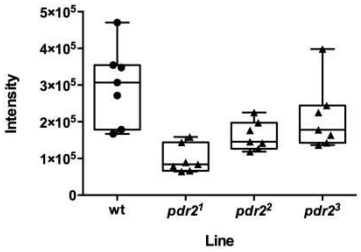
Petuniasterone H (521.3473, $[M+H]^+$)	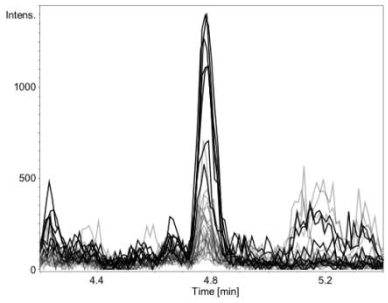	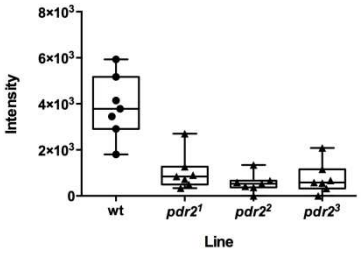
Petuniolide E (487.3055, $[M+H]^+$)	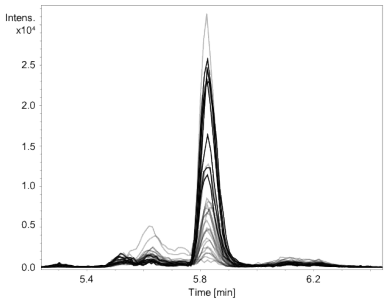	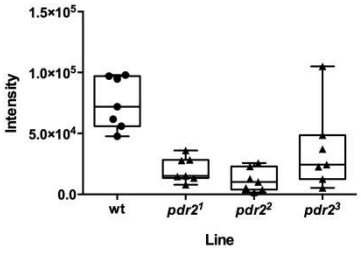
K-3-GluGal (609.1462, $[M+H]^-$)	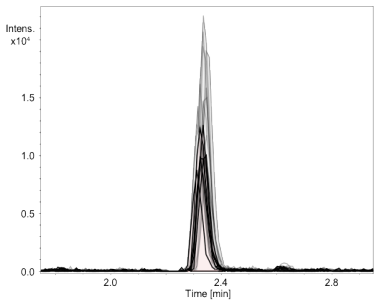	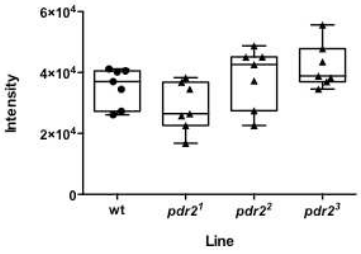
Q-3-GluGal (625.1410, $[M+H]^-$)	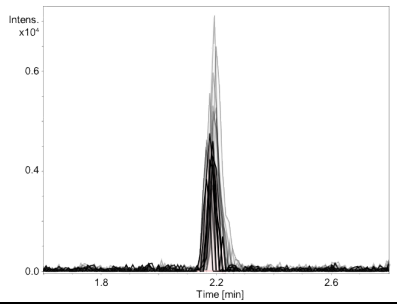	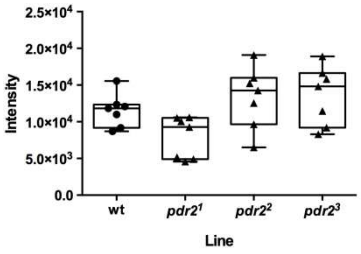

Extracted ion chromatograms (EICs) and Box-Whisker plots of selected metabolites found in wild-type (wt, black) and *pdr2* (grey) lines of experiment 2, showing a reduction of petuniasterone and petuniolide contents and an unchanged intensity of flavonoids in *pdr2* lines . Structures were drawn according to literature (Elliger et al. 1988a; Elliger et al. 1989a; Zerback et al. 1989; Elliger and Waiss 1991). Q-3-GluGal: Quercetin 3-*O*-(2''-*O*-*β*-D-glucopyranosyl)-*β*-D-galactopyranoside. K-3-GluGal: Kaempferol 3-*O*-(2''-*O*-*β*-D-glucopyranosyl)-*β*-D-galactopyranoside (Zerback et al. 1989).

Supplemental Table 2. XCMS analysis of content reduction of unknowns metabolites in *pdr2* lines

Substance	Feature ID	Fold[1)]	p-value (≤ 0.01)	m/z_{med}	m/z_{theo}	Accuracy [ppm]	Chemical Formula	Rt_{med} (min)	Intensity (≥ 1000)	Adduct / Fragment
unknown	#6	0.46	1.09E-05	481.2951				5.63	2878	[M+H]+
	#131	0.38	2.52E-03	421.2734				5.64	1970	[M+H-AcOH]+
	Avg:	**0.42**	**1.27E-03**	–	**–**	**–**	**–**	–	**4848**	= Σ intensities
unknown	#116	0.40	2.13E-03	531.3309				5.46	1238	
	#109	0.47	1.84E-03	547.3255				5.46	1282	
	Avg:	**0.43**	**1.98E-03**	–	**–**	**–**	**–**	–	**2520**	= Σ intensities
unknown	#146	0.47	2.85E-03	265.1597				6.26	1506	$[M+H-AcOH]^+$
	#277	0.42	6.39E-03	325.1795				6.26	10508	$[M+H]^+$
	Avg:	**0.44**	**4.62E-03**	–	**–**	**–**	**–**	–	**12014**	= Σ intensities
unknown	#25	0.33	1.37E-04	1182.6822				5.83	1929	
	#418	0.13	9.75E-03	1032.6404				5.83	1920	
	Avg:	**0.19**	**4.95E-03**	–	**–**	**–**	**–**	–	**3849**	= Σ intensities
unknown	#199	0.41	4.23E-03	465.3008				6.25	5654	$[M+H]^+$
	#267	0.43	6.10E-03	405.2790				6.25	4836	$[M+H-AcOH]^+$
	Avg:	**0.42**	**5.17E-03**	–	**–**	**–**	**–**	–	**10490**	= Σ intensities
unknown	#179	0.39	3.50E-03	285.1478				5.23	1001	
	#313	0.43	7.15E-03	575.2667				5.23	4688	$[M+H]^+$
	#296	0.42	6.80E-03	592.2931				5.23	25719	$[M+NH_4]^+$
	#286	0.44	6.50E-03	597.2485				5.23	4285	$[M+Na]^+$
	Avg:	**0.42**	**5.99E-03**	–	**–**	**–**	**–**	–	**35693**	= Σ intensities
unknown	#239	0.20	5.39E-03	575.3023				4.22	1292	$[M+H-2H_2O]^+$
	#406	0.21	9.46E-03	593.3129				4.22	1943	$[M+H-H_2O]^+$
	#344	0.17	7.93E-03	611.3238				4.22	14396	$[M+H]^+$
	#401	0.20	9.41E-03	628.3502				4.22	4940	$[M+NH_4]^+$
	Avg:	**0.19**	**8.05E-03**	–	**–**	**–**	**–**	–	**22571**	= Σ intensities
unknowns with unique mass	#74	0.65	1.07E-03	639.2859				6.04	1087	
	#85	0.44	1.33E-03	561.3074				5.32	2136	
	#92	0.54	1.46E-03	629.3672				6.02	1169	
	#174	0.34	3.43E-03	519.2951				4.38	1256	
	#179	0.39	3.50E-03	285.1478				5.23	1001	
	#189	0.52	3.81E-03	639.2948				5.67	2826	
	#195	0.43	4.16E-03	599.3028				6.26	9874	
	#206	0.35	4.38E-03	696.3076				6.60	1633	
	#253	0.40	5.86E-03	441.2634				5.07	2124	
	#341	0.46	7.91E-03	571.3259				6.62	1389	
	#394	0.43	9.23E-03	610.3036				4.56	28022	

The description of the experiment can be found in Table 1. Metabolites with intensities >1000 and a significant reduction are displayed in order of decreasing p-value.

Supplemental table 3: characteristics of metabolites quantified in leaf extracts		
Metabolite	t_R	**EICs considered for Quantification**
Petuniasterone A acetate	9.14	601.3194 , 618.3459 $[M+NH_4]^+$, 623.3013 $[M+Na]^+$
Petuniolide E	8.22	427.2843 $[M+H–AcOH]^+$, 487.3054 $[M+H]^+$, 504.320 $[M+NH_4]^+$, 509.2874 $[M+Na]^+$
Petuniolide F1	7.83	503.3003 $[M+H]^+$, 520.3269 $[M+NH_4]^+$, 525.2823 $[M+Na]^+$
Petuniolide F2	7.07	503.3003 $[M+H]^+$, 520.3269 $[M+NH_4]^+$, 525.2823 $[M+Na]^+$
Petuniolide F3	7.30	503.3003 $[M+H]^+$, 520.3269 $[M+NH_4]^+$, 525.2823 $[M+Na]^+$
Petuniolide F4	7.20	503.3003 $[M+H]^+$, 520.3269 $[M+NH_4]^+$, 525.2823 $[M+Na]^+$
Petuniasterone G*	7.78	461.3262 $[M+H]^+$
Petuniolide C	6.93	441.2636 $[M+H–AcOH]^+$, 501.2847 $[M+H]^+$, 523.2666 $[M+Na]^+$
Petuniasterone J	7.62	601.3371 $[M+H]^+$, 618.3637 $[M+NH_4]^+$, 623.3191 $[M+Na]^+$
Petuniasterone H	7.36	521.3473 $[M+H]^+$, 543.3292 $[M+Na]^+$
Petuniasterone I/P3	6.57	633.3092 $[M+H]^+$
Petuniasterone I/P3	7.91	633.3092 $[M+H]^+$, 650.3357 $[M+NH_4]^+$, 655.2911 $[M+Na]^+$
Petuniolide A	7.50	425.2686 $[M+H–2AcOH]^+$, 485.2898 $[M+H–AcOH]^+$, 545.3109 $[M+H]^+$, 562.3374 $[M+NH_4]^+$, 567.2928 $[M+Na]^+$
Petuniasterone L/R	7.97	615.2986 $[M+H]^+$, 632.3252 $[M+NH_4]^+$, 637.2806 $[M+Na]^+$
Petuniasterone L/R	8.06	597.2867 $[M+H–H_2O]^+$, 615.2986 $[M+H]^+$, 632.3252 $[M+NH_4]^+$, 637.2806 $[M+Na]^+$
Perulactone C/D	–	535.3265 $[M+H]^+$, not detected
Corticosterone (ISTD)	5.76	347.2217 $[M+H]^+$, 369.2036 $[M+Na]^+$, 387.2142 $[M+Na+H_2O]^+$

*) Only one Petuniasterone G could be detected